

PLACE IN RETURN BOX to remove this checkout from your record.
TO AVOID FINES return on or before date due.
MAY BE RECALLED with earlier due date if requested.

DATE DUE	DATE DUE	DATE DUE
JUN 18 2003		

**MODEL FOR PREDICTING APPLICATION TORQUE AND REMOVAL TORQUE
OF A CONTINUOUS THREAD CLOSURE**

By

Supachai Pisuchpen

A THESIS

**Submitted to
Michigan State University
in partial fulfillment of the requirements
for the degree of**

MASTER OF SCIENCE

2000

ABSTRACT

MODEL FOR PREDICTING APPLICATION TORQUE AND REMOVAL TORQUE OF A CONTINUOUS THREAD CLOSURE

By

Supachai Pisuchpen

Classical engineering mechanics is applied in the analysis of the closure-container system. The basic assumption that the system can be modeled as a rigid-body leads to the TLRD method for determining the static coefficient of friction of a closure-container system (μ_s , μ_t) and the predictive models for the application torque and the removal torque. The static coefficients of friction were measured for six closures and seven liners. The discrepancy found between theoretical predictions of torque and experimental results is attributed to the inability of the models to account for the viscoelastic properties of the liner materials as a result of the damping effect. The “f factor” or the sealing force ratio derived from the spring & dashpot model of the liner materials is a good indicator for determining the capability of the liner materials to hold the sealing force. Modifications to the predictive models by incorporating the viscoelastic behavior are suggested.

**Copyright by
SUPACHAI PISUCHPEN
2000**

ACKNOWLEDGMENTS

As ever, this research wouldn't be accomplished without encouragement and guidance. I gratefully acknowledge the expertise, valuable advice and tolerance of Dr. Hugh Lockhart, Dr. Gary Burgess, and Dr. Gary Cloud.

I also wish to thank Bob Hurwitz who inspired me and gave valuable suggestions in developing the testing device.

I heartily thank my parents for their interest, support and encouragement to my judgement in goal of life.

Last but not least, I would like to acknowledge this latest of many debts to my beloved wife, Wariya, who temporarily lost a husband to a research. I can not thank her enough for her patience and understanding.

TABLE OF CONTENTS

LIST OF TABLES	vi
LIST OF FIGURES	vii
LIST OF ABBREVIATIONS.....	ix
1. INTRODUCTION	1
2. LITERATURE REVIEW	4
3. MATERIALS AND METHODS	19
4. RESULTS	42
5. CONCLUSIONS	57
APPENDIX-RAW DATA TABLES	60
BIBLIOGRAPHY	124

LIST OF TABLES

1. The Static Coefficient of Friction from Robert V. McCarthy's Experiment.....	18
2. Details of Bottles Used in the Research.....	19
3. Details of Closures Used in the Research	20
4. Summary of the Dimension Parameters of Various Treatments Tested	42
5. Static Coefficient of Friction at the Thread Interface, μ_t , $n = 5$	44
6. Static Coefficient of Friction at the Liner Interface, μ_s , $n = 5$	45
7. Comparison of the Predicted Removal torque, T' and the Measured Removal Torque, ISRT, and IRT.....	49
8. Comparison of T'/T and ISRT/AT, and the "f Factor" or sealing force ratio ..	53
9. Comparison of T'/T and IRT/AT, and the "f Factor" or sealing force ratio	53
10. Raw Data of the Static Coefficient of Friction at the Thread Interface.....	60
11. Raw Data of the Static Coefficient of Friction at the Liner Interface	90
12. Raw Data of the Measured Application Torque and Instantaneous Removal Torque	117
13. Raw Data of the Measured Application Torque and Immediate Removal Torque	119
14. The Predicted Removal Torque, T' Calculated Using AT from Table 12.....	121
15. The Predicted Removal Torque, T' Calculated Using AT from Table 13.....	121
16. k_a and k_r for Equations (18) and (19)	122

LIST OF FIGURES

1. The Most Popular Finish Designs of CT Closure	5
2. Standard Code Letters for Continuous Thread Plastic.....	6
3. Plastic Container Thread Profiles.....	8
4. The Structure of F-217 Liner.....	13
5. Force Field of Screw Thread.....	14
6. Torque-Friction Tester and the Concept	18
7. The Conceptual Design for Measuring the Static Coefficient of Friction of Closure-Container System.....	24
8. Free-Body Diagram of the Liner and Finish in Contact	25
9. Free-Body Diagram of the Closure Thread and Container Thread in Contact.....	27
10. The Treatments Tested for the Static Coefficient of Friction at the Thread Interface.....	29
11. The Treatments Tested for the Static Coefficient of Friction at the Liner Interface.....	30
12. Free-Body Diagram of the Closure-Container System.....	34
13. Relative Magnitude of Torque Contributed by Thread and Liner Factor	35
14. The Spring-Dashpot Model for Liner Materials under Compression	38
15. The “L” and “M” Thread Profiles Obtained from the Unscrewing and Stripping Mold.....	43
16. Comparison of ISRT and T'	50
17. Comparison of IRT and T'.....	50

18. Comparison of the “f factor” 10 sec and 15 min after Application	55
--	----

LIST OF ABBREVIATIONS

C.T.	=	Continuous Thread
TIP	=	Torque Inch Pounds
TLRD	=	Top Load/Rotation/Deadweight Loading
AT	=	Application Torque
RT	=	Removal Torque
ISRT	=	Instantaneous Removal Torque
IRT	=	Immediate Removal Torque
Avg	=	Average
Sd	=	Standard deviation

1. INTRODUCTION

A closure system is a mechanical device that seals the contents within a container and can be removed to allow the contents to be dispensed. A closure is applied to the “finish” of a glass, metal, or plastic container. It is an important part of the container in maintaining integrity of the packaging system throughout the entire process of storage, picking and packing. The security of the closure depends upon a number of variables such as resiliency of liner, flatness of seal surface on the container, and the most important; tightness or torque that it is applied. Torque is a moment or twisting resistance that occurs during the application or removal of a closure on a container. Application torque is a measure of closure tightness created by the contact between a closure and a container, whereas removal torque is a measure of the amount of moment or twisting effort necessary to loosen while attempting to open it.

The literature review on the prediction of closure torque indicates that there are not many works published in this area. In addition, most of the published research on removal torque has been done on varieties of closure and environment systems rather than development of a predictive model. As a matter of fact, the latter area is as important and challenging as the former for the investigators to unveil the phenomena hidden in the closure during exposure to the environment.

This study was initiated to develop a model for predicting torque of a continuous thread closure. The model will deal with forces and moments, and the effects of forces and moments acting on rigid bodies at rest. This study is the

first step in developing a more complicated model reflecting the actual conditions to which a closure system is susceptible in the environment. The closure system engaged with a container can be viewed as a mechanical system to clearly understand how it functions to provide a seal protection for the product. The continuous threaded closure-container system is a torque dependent system. The seal is usually accomplished through the use of a liner in a cap which is applied with the proper amount of torque. The liner performs like a gasket to seal around the finish. When the closure is properly applied, the liner is under compression and reacts like a spring to keep the closure thread in contact with the bottle threads and to secure the closure of the container. The closure-container system thus functions through the interaction of many factors which include sealing force, torque and other characteristics of threaded closures.

There are two main goals of this study. The first one is to establish the method of determination of two static coefficients of friction; one between thread of closure and thread of container and another between liner and finish of container. This goal is important for developing a predictive model since currently there is no means yet to determine the parameters, and a static coefficient of friction mainly depends on types of material in contact, and types of surface. The second goal is to develop a static model for predicting torque of a continuous thread closure. This development of a predictive model is based on a static equilibrium, which has no movement and deformation; it does not associate with time and environment factors e.g. temperature, humidity. In fact, temperature and humidity fluctuations and their extremes in storage and

transportation can affect removal torque. In addition, shock and vibration from handling or shipping and compression or top loading from storage also exist and influence closure tightness as well. Understanding this model is very useful for explanation of the translation of torque into sealing force, the effect of friction, and the closure performance.

It is expected that the information from this study will be extended to develop a model associated with time and environment factors, which describe the closure-container systems when exposed to actual conditions.

2. LITERATURE REVIEW

1. Continuous thread closure

The advent of continuous thread closures arose from a Philadelphian named Espy who conceived the idea of affixing a disc of cork inside the cap so when screwed down on the neck of the jar, the cap brought the cork in compressing contact around the mouth. The Espy patent issued in 1856 could have been a landmark in closure history. However, there were deficiencies in sealing effectiveness of the first design of thread. This brought inventors to consider development in this area. In 1858, John L. Mason was granted patents for his improved thread and improved mold for blowing bottles with threads. His idea was to start a diagonal thread slightly below the top and let it fade away before reaching the shoulder. After this improvement, many materials were used in the closure and bottle industry, accompanied by the continuous improvement of closure design. In 1927, plastic closures were introduced with a promise of freedom of design e.g. colors, textures. As the new technology in resin improvement became available, and more suitable for specific purposes, the variety of products packed with plastic closures drastically increased. In basic principle, the threads of the screw closure engage with corresponding threads molded on the neck of the container; this style offers a mechanical means of generating force for effective sealing. Acceptable mechanical properties and protection can be accomplished by the use of plastic continuous thread closure. Therefore, it has become a principal type of closure.

To standardize the dimensions and terms used in the closure industry, the Closure Manufacturers Association has prepared a guide and standard for both metal and plastic closures. By definition, a continuous thread (C.T.) closure has a spiral thread, the design of which is tailored to the container finish and its thread. Hence, a closure is retained on a container by threads that engage corresponding threads of the container. Single lead threads having one thread with a single start are the most common. The size and type of thread are usually designated by the diameter in millimeters coupled with a number which signifies the finish style, such as shallow, deep. Thus 28-400, or sometimes written, 400-28 means 28 mm in major diameter and a shallow continuous thread. Series designations for the most popular C.T. closures are 400 and 425 for shallow continuous thread designs, 410 for medium CTs, and 415 for tall CTs (Figure 1).

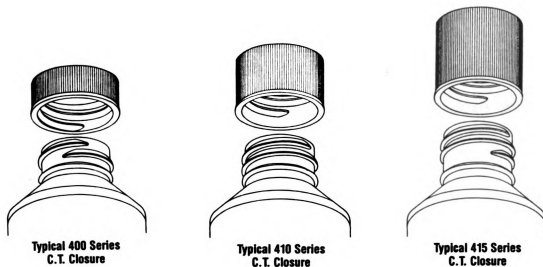


Figure 1. The Most Popular Finish Designs of CT Closure

Source: The Closure Manufacturers Association, 1993, Closure Guides

A cross section of the continuous thread closure shows the basics of closure construction in Figure 2.

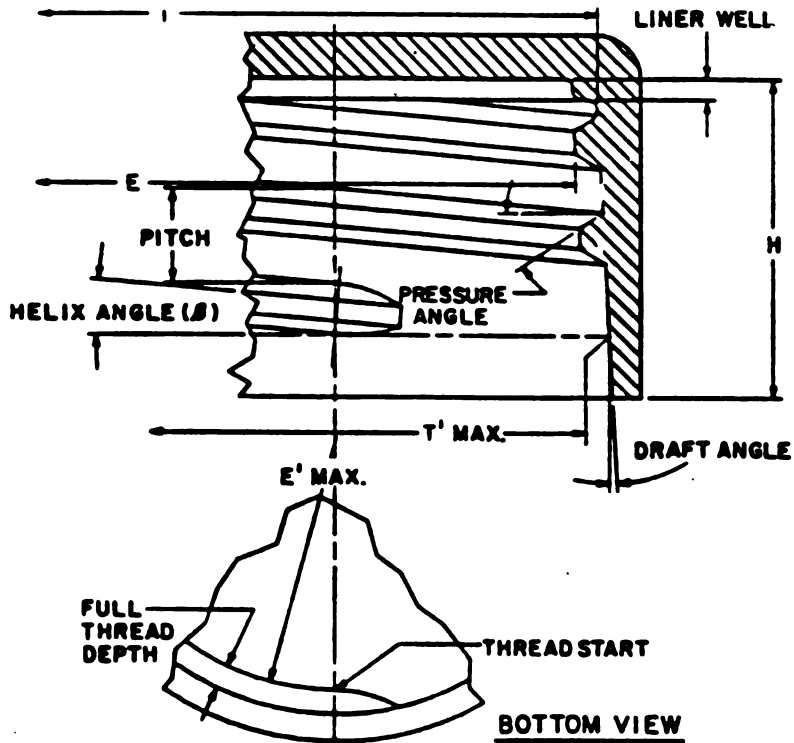


Figure 2. Standard Code Letters for Continuous Thread Plastic closures

Source: The Closure Manufacturers Association, 1993, Closure Guides

where	E	= Minor diameter of thread
	E' MAX	= Similar to E, allows for molding draft angle.
	T	= Major diameter of thread
	T' MAX	= Similar to T, allows for molding draft angle.
	H	= Vertical distance from bottom of closure to the inside top surface
	β	= Helix angle

**PITCH = Vertical distance between corresponding points
on adjacent threads.**

The important closure dimension terms to recognize and understand are defined by the Closure Manufacturers Association in the Closure Guides and described as follows:

1. T dimension, and E dimension. T is the major diameter of the thread on a C.T. closure, whereas the minor diameter of the thread on a C.T. closure is E. The T and E dimensions are measured at the top of the closure at a point near the end of full thread.
2. H dimension. The vertical distance between the inside top of the closure at the sealing area and the bottom of the skirt excluding any liner (if used), or linerless, or any other sealing elements.
3. Helix angle (β). The inclination angle made by the spiral of the thread in relation to the horizontal axis is the helix angle.
4. Pitch. Pitch is the distance from any one point on a closure thread to the corresponding point on the next thread. Thus, pitch is also equal to the inverse of threads per inch.
5. Pressure angle. The angle of the tangent line at the point where the closure thread contacts the finish thread. This is also known as the bearing angle.
6. Threads per inch (T.P.I). T.P.I. is the number of threads in a distance of an inch. It is also equal to 1 divided by pitch.

The next issue to be considered in this study is plastic container thread profiles. Although voluntary standards for plastic closure thread profiles have not been developed yet, there are 3 standard container thread profiles (Figure 3).

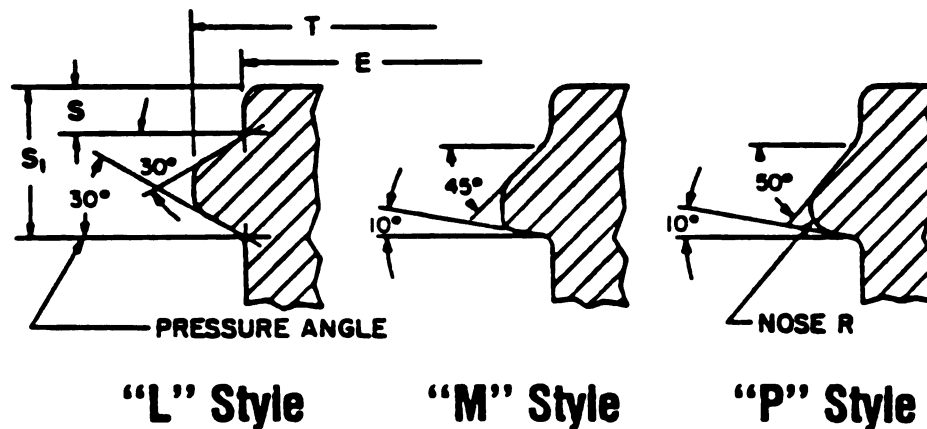


Figure 3. Plastic Container Thread Profiles

Source: The Closure Manufacturers Association, 1993, Closure Guides

Closure manufacturers have modified these standard container threads into their closure designs along with variations of each. The closure sizes are usually designed in accordance with the finish size of the container. For example, if the finish size of the container has diameter of 28 mm., the 28 mm. diameter of the closure is needed to fit this container. However, the closure thread profiles modified from the container thread profiles have often been used without relation to a specific container finish thread. In Figure 3, L style is designated as an all-purpose thread for either plastic or metal closures and has a symmetrical 30° pressure angle. M style is a modified buttress type with 10°

pressure angle which is the preferred style for plastic containers and is used exclusively for this purpose, whereas P style is similar to M style, except it has a full nose radius for use on certain pour-out finishes. Thus, plastic closure thread profiles are designed to fit one of these three container thread profiles.

Thermoplastic materials are mostly used in manufacturing C.T. closures. Most often polyolefins (e.g. polypropylene, polyethylene) are used but there is some use of polystyrene. Each of these materials has specific properties that influence the choice of thread profile, and the performance of closure.

1. Polyethylene. PE is available in three densities: LDPE, MDPE, and HDPE.

As density increases, the material becomes stiffer, glossier, and harder, and also the tensile strength increases. HDPE is used for manufacturing containers more than for closures.

Advantages	Limitations
a. Flexibility allows for undercuts	a. Limited heat resistance
b. Remains flexible over wide temperature range.	b. Low abrasion resistance
c. Good moisture and chemical barrier	c. Low barrier to oils, gases, flavors and odors.
d. Good processability	d. Stress cracking
e. Heatsealable	e. Deform under loading, creep
f. Wide range of available colors	f. May be degraded by UV
g. Variety of surface finishes is possible.	

Source: The Closure Manufacturers Association, 1993, Closure Guides

2. Polypropylene. PP has unusually high resistance to stress cracking. This is an essential characteristic for hinged closures. In thin hinged sections, it has the quite remarkable property of strengthening with use. Thus, plastic closures are widely made from PP.

Advantages	Limitations
a. Higher heat resistance than PE	a. Embrittle at low temperature
b. Flexible enough for certain undercuts.	b. Limited abrasion and creep resistance
c. Excellent moisture barrier	c. Poor gas barrier
d. Good chemical resistance	d. Limited stress cracking resistance
e. Good processability	e. May be degraded by UV
f. Stiffer and harder than PE	
g. Wide range of available colors	
h. Low weight per unit volume	

Source: The Closure Manufacturers Association, 1993, Closure Guides

2. Liner

The closure liner, a material that creates a seal between the closure and container, is critical in maintaining the quality of product and the integrity of the seal on the container. The selection of the closure liner on a product-container system can make the difference between the success and failure of a product.

The liner is composed of two major parts: a backing and a facing.

Compressibility, resiliency, and resealability are provided by the backing, whereas the facing directly contacting a product provides barrier protection.

There are variables that should be considered when selecting the closure liner for a certain product (Source: Crawford, Brian, Choosing the Right Closure Liner). These variables can be categorized as follows:

1. **Product compatibility.** A liner should be compatible with a closure and a product. Basically, liner should be chemically inert to the product and resistant to container's content in compliance with the FDA regulations.
2. **Macro seal.** Physically, the liner must compensate for imperfections on the container's lip and on the closure in order to prevent the leakage of the product.
3. **Micro seal.** This means a seal against small molecules such as water vapor, gas, flavor and odor. Loss of barrier protection characteristics has direct results in product deterioration. Therefore, the loss of these chemical molecules or the entering of environmental components from outside into the container must be impeded.
4. **Application and removal torque.** They are partly related to the coefficient of friction between thread of closure and thread of container, and between the liner and container finish. Ideally, the amount of friction should facilitate the capper in application and consumer in removal without backing off during transportation. In addition, the torque is also related to compression and tensile stress behavior in container finish, closure and liner.
5. **Other considerations.** In some applications, particular properties may be needed, for instance, heat resistance, tamperproofing.

Materials used for closure liners can be grouped into two categories: homogeneous and heterogeneous composition. The use of a single material in the liner is defined as homogeneous; heterogeneous refers to the incorporation of two or more different materials. Recently, combinations of materials in liners especially extruded polymers have become widely used because new technology allows customizing properties needed from one material and combining with other materials. Some of the commonly used combinations (backing/facing) are:

polyethylene/EVA/polyethylene

polyethylene/foamed polyethylene/polyethylene

polyethylene/foamed EVA/polyethylene

high density polyethylene/foamed low density polyethylene

/high density polyethylene

polypropylene/foamed low density polyethylene/polypropylene

acrylonitrile/polyethylene

pulp/Saran film

pulp/polyvinyl lubricant film

pulp/polyethylene coated paper

In 1972, F-217 liner was developed by Tri-Seal. This patented seal is a coextruded structure: a low density polyethylene foam core sandwiched between two layers of low density polyethylene film (Figure 4).

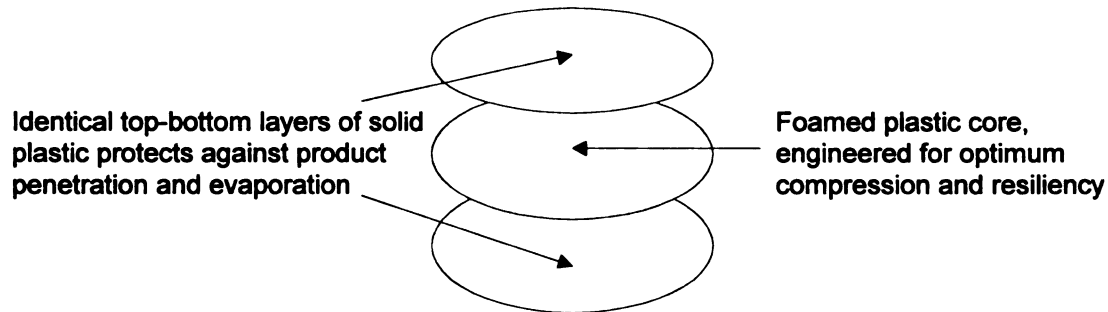


Figure 4. The Structure of F-217 Liner

F-217 is one of the most popular lining materials used in the market. It is a general-purpose liner and is recommended for sealing household, cosmetic, liquor, drug, food, and other products.

Pulpboard, a backing material, waxed, coated with varnish, or laminated to plastic films were the first combination materials used for liners. Varnished pulp liners offer good resistance to heat and chemicals, low water-vapor transmission and a glossy appearance, but they tend to be brittle. Thermoplastics such as vinyl, Saran, and polyethylene are also good choices for laminating or coating on pulp as facing materials. The selection of type of coating is dependent on what protections are needed. For instance, polyethylene is a good moisture protection but inferior in barrier to most gases. So it is not suitable for oxygen-sensitive products.

$$T = F_v \cdot r \cdot \frac{\cos \theta \cdot \sin \alpha + \mu \cdot \cos \alpha}{\cos \theta \cdot \cos \alpha - \mu \cdot \sin \alpha} \quad (1)$$

$$T' = F_v \cdot r \cdot \frac{\mu \cdot \cos \alpha - \cos \theta \cdot \sin \alpha}{\mu \cdot \sin \alpha + \cos \theta \cdot \cos \alpha} \quad (2)$$

where

T = the necessary torque to develop a particular holding
or sealing force

T' = the torque required to remove the threaded attachment

F_v = the sealing force (axial force)

μ = the coefficient of friction at the thread interface

α = thread helix angle

θ = contact angle

In fact, these expressions were originally developed by similar summations of forces and moments of loaded closures in Boomsliter (1945).

One limitation of these expressions in predicting removal torque or sealing force effectively is the assumption that all parameters remain constant during loading. In fact, relaxation of the liner material causes the sealing force to decay and must be included in the design of the closure screw thread. McCarthy reported that the relaxation of plastic material associated with the closure skirt amplifies the sealing force decay. The investigator developed further mechanical models to simulate the major relaxation mechanism affecting the observed sealing force decay. The model compared favorably with actual data. This research, however, did not include the effect of liner behavior in the model.

Technically, torque depends mostly on the behavior of the closure liner rather

than the threads. Therefore, the model does not quite represent the actual static equilibrium of the closure-container system.

There is no other research reported in this area since 1956 while the technology in material and packaging machinery has been developing continually. However, there was some research conducted to investigate various effects on the removal torque of closure. Most was conducted by Dr. Lockhart of the School of Packaging at Michigan State University and Dr. Greenway of University of Missouri-Rolla.

McCarthy's research leaves an important aspect of closure-container systems unanswered. As mentioned above on the effect of the liner, this research continues the analysis of the effect of the liner further by using the static equilibrium approach.

4. Coefficient of friction

Frictional behavior is important in many packaging applications involving banding of unitized loads, lifting of packages, abrasion or scuffing. In addition, the coefficient of friction plays a major role in the torque of the closure. Friction is a measure of the force that resists the motion of one surface against another surface. Furthermore, the force required to start the object moving is related to the static coefficient of friction, while the kinetic coefficient of friction is related to the force required to maintain motion. Fundamentally, the kinetic coefficient of friction is always less than the static coefficient of friction because force to keep the object moving is less than force to start the object moving. There are many

factors affecting the coefficient of friction. They can be classified into two categories. External factors include those such as temperature, velocity of sliding, and load. Internal factors involve nature of the contact surface (smooth or rough), nature of the materials, presence or absence of lubricants.

To apply a predictive model in the design of the continuous thread closure, an appropriate value of the static coefficient of friction is necessary. A great variety of instruments have been developed to measure coefficient of friction from a simple inclined plane to complex apparatus. Precise values of static coefficient of friction for the application of closures are not currently available for particular plastics on container materials (e.g glass, metal, plastics). McCarthy developed a technique to simulate friction conditions for a closure screw thread. The method employed a spring clamp of known k (spring constant) and a closure of the subject material cut to relieve resistance to deformation in one diameter (d) for a distance of at least 0.06" (Figure 6).

The jaws of the clamping unit were faced with neoprene. The torque-friction tester was applied to a loose fitting closure. By applying a clamping force generated by the spring, the spring compression force was a direct reading of the radial force applied to the closure. The rotation of torque-friction tester would unscrew a closure from a contact material (bottle), then the torque reading was recorded. The coefficient of friction could be experimentally determined using a relationship of $T = \mu \cdot F_c \cdot d$.

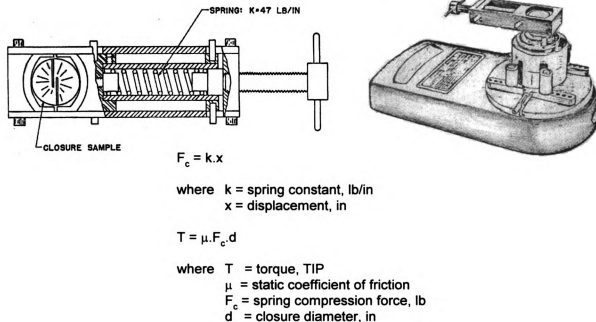


Figure 6. Torque-Friction Tester and the Concept

The static coefficients at thread interface obtained from McCarthy's experiment are summarized in Table 1.

Table 1. The Static Coefficient of Friction from Robert V. McCarthy's Experiment

Materials in contact	μ
Polypropylene on glass	0.08
Polystyrene on glass	0.28
Linear low density polyethylene on glass	0.08

3. MATERIALS AND METHODS

1. Materials and instruments

1. The closure-container systems

The systems were categorized into 2 groups; 28 mm and 38 mm diameter.

Tables 2 and 3 show the details of the bottles and closures tested.

Table 2 Details of Bottles Used in This Research

Designation	Finish size-style, mm	Material	Description
A*	20-410	HDPE	Brick red color, round shape, made by Owen-Brockway Plastics & Closures, received 10/1/97
B	28-400	HDPE	White color, 60 ml volume, square shape, made by Owen-Brockway Plastics & Closures, received 08/25/99 <ol style="list-style-type: none">1. Machine #482. Mold #54373. Product #25-006-024
C	38-400	HDPE	White color, 100 ml vol , square shape made by Owen-Brockway Plastics & Closures, received 10/8/96

Note: A* was eliminated from this research because the static coefficient of friction could not be measured using the TLRD method.

Table 3 Details of Closures Used in This Research

Designation	Finish size-style, mm	Closure material	Liner material	Description
A1*	20-410	PP	PE foam (F-217)	FRST PP WH 7135 PE FM, white color, made by Poly-Seal Corporation, received 10/1/97
B1	28-400	PP	PE foam (OB-Seal)	Fine rib closure, prod##lot# 992526, white color, glued 1. outer cap-Philips HLN-120: (OIP 32699) 2. the lining mat is 0.040 PL-4025 OB seal/ lot # 151171 3. Colorant: white OIC #60110 made by Owen-Illinois, received 11/17/99
B2	28-400	PP	PE foam (OB-Seal)	Fine rib closure, white color, hand lined, non-glued, made by Owen-Illinois, received 11/22/99
B3	28-400	PP	PE foam (OB-Seal)	Fine rib closure, black color, hand lined, non-glued, made by Owen-Illinois , received 11/22/99
B4	28-400	PP	Pulp/Saran(P/SF)	Fine rib closure, black color, hand lined, non-glued, made by Owen-Illinois , received 12/01/99
B5	28-400	PP	Pulp/Saran(P/SF)	Fine rib closure, white color, hand lined, non-glued, made by Owen-Illinois , received 12/01/99

Table 3 (cont'd)

B6	28-400	PP	Pulp/Polyvinyl lubricant film(P/RVTLF)	Fine rib closure, black color, glued, made by Owen-Illinois, received 11/26/97
B7	28-400	PP	Pulp/Polyvinyl lubricant film(P/RVTLF)	Fine rib closure, white color, hand lined, non-glued, made by Owen-Illinois, received 11/22/99
B8	28-400	PP	Pulp/Polyvinyl lubricant film(P/RVTLF)	Fine rib closure, white color, hand lined, non-glued, made by Owen-Illinois, received 11/22/99
C1	38-400	PP	PE foam (F-217)	Fine rib closure, white color, glued, made by Poly-Seal Corp, received 11/12/94
C2	38-400	PP	PE foam (OB-Seal)	Fine rib closure, white color, hand lined, non-glued, made by Owen-Illinois, received 12/01/99

Note: A* was eliminated from this research because the static coefficient of friction could not be measured using the TLRD method.

- 2. Secure Pak torque tester electronic model (digital display)**
- 3. Mitutoyo digimetric caliper**
- 4. Bridgeport comparator**
- 5. Clear casting resin and polyester catalyst for making closure specimens for cross-sectional measurement**

6. An instrument developed for determining the static coefficient of friction of the closure-container systems.

2. Methods

1. Cross-sectional measurement of the closure-container system

Duplicate of treatments in Figure 10 applied on the similar diameter containers were tested. A closure was applied on the container with the prescribed application torque of 14 TIP for 28 mm diameter closure and 19 TIP for 38 mm diameter closure. Then a closure-container system was placed upside down into the prepared box 3x3x1.25 inches (the inside surface of the box was covered with pressure sensitive tape). The clear casting resin and the polyester catalyst were thoroughly mixed and poured into the prepared box. This step was performed in the hood. The box was cured in the hood until the casting was completely dry, after which the casting was removed from the box. Finally, the casting was cross-sectioned using a band saw and polished to make a smooth clear surface. The measurements of T, E, I, and the angles α and θ were made using the optical comparator. On the bottles, the T dimension is the major diameter of the bottle finish including the threads. The E dimension of the bottle is the minor outside diameter of the bottle finish excluding the threads. The diameter at the smallest opening inside the finish is the I dimension. The angle α is the incline angle made by the spiral of the thread in relation to the horizontal plane measured at the mean diameter of the thread interface. Finally, the angle θ is the contact angle between the closure threads and the container

threads measured along the vertical axis. The illustrations of these parameters are shown in Figures 2 and 9a

2. The static coefficient of friction measurement

This research began with the use of McCarthy's concept for measuring the static coefficient of friction at the thread interface. A clamping unit similar to McCarthy's was fabricated and used. However, the static coefficient of friction measured this way was very dependent on the speed of rotation, either clockwise or counterclockwise. The data obtained were scattered and unrepeatable.

The results dictated the development of a better means which is simple, controllable, and repeatable. The method developed in this research allows for measuring the static coefficient of friction at the thread interface, and at the liner interface regardless of the speed of rotation and the twisting direction. The concept of the experimental setup is shown in Figure 7. The closure is attached to a circular plate. The forces applied on both sides of the circular plate are just sufficient to initiate sliding of the closure on the container at the contact point, while the top load exerts a downward force on the closure. This conceptual design was carried on to develop the testing device in Figure 7 which allows placement of a top load on the closure while applying an increasing torque by means of deadweight loading a string and pulley system. For convenience, this device is named Top Load/Rotation/Deadweight Loading Device. The short name for it is TLRD. The results show that the method gives repeatable results

under various experimental conditions. In general, friction forces involved when two bodies are in contact can be examined by the static equilibrium approach. Beginning with a simple system, a static coefficient of friction between the liner surface and the finish of the container is considered before stepping up to a more complicated system.

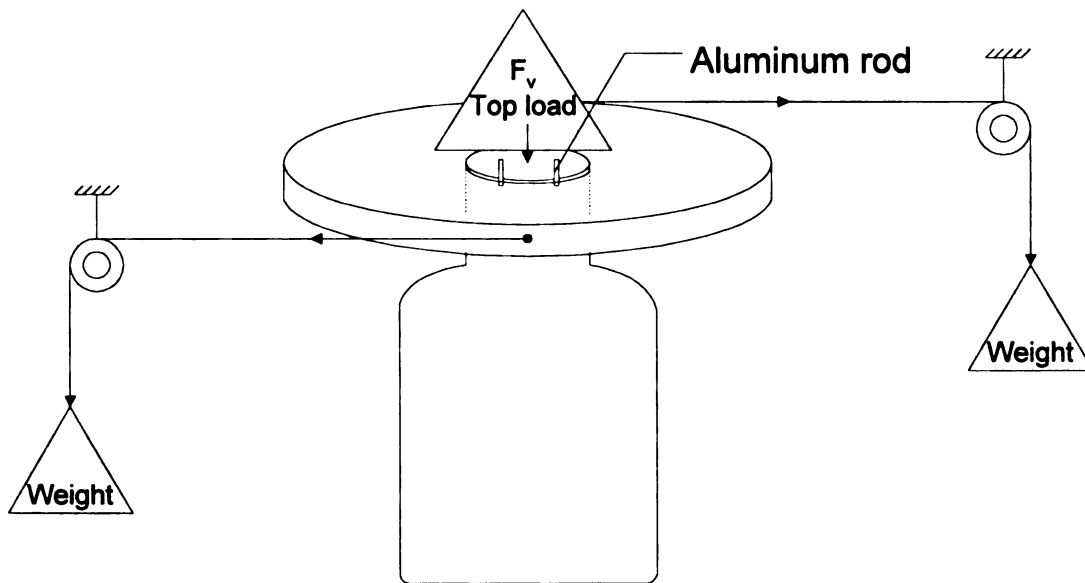


Figure 7 The Conceptual Design for Measuring the Static Coefficient of Friction of Closure-Container Systems (TLRD Method)

To determine the static coefficient of friction at the liner interface, the threads around the container neck have to be eliminated. Thus, the only contact is between the liner and the finish of the container. A free-body diagram showing the forces acting on the liner and finish in contact is given in Figure 8. It shows that the top load F_v in Figure 7 vertically pushes the liner surface against the

finish of the container, and the normal force F_n is the reaction exerted on the liner at the points of contact to balance the force F_v shown in Figure 8.

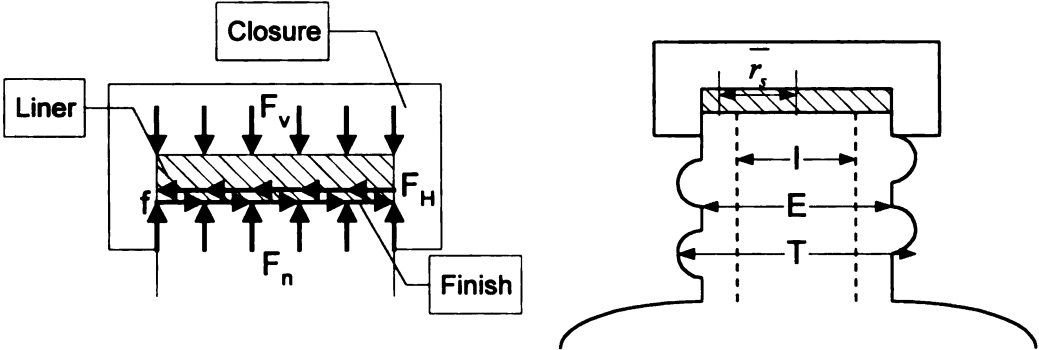


Figure 8 Free-Body Diagram of the Liner and Finish in Contact

These forces are equal but in opposite directions, and are present whenever the bodies are in contact, whether or not there is any tendency for one to slide relative to the other. Thus, a force balance in the vertical direction produces the equation.

$$\sum F_y = 0, \quad F_v = F_n \tag{3}$$

When a torque is applied to the closure, there is a tendency for the liner to slide over the finish. The finish exerts frictional forces, f on the liner all around the rim of the container.

$$\sum F_x = 0, \tag{4}$$

From symmetry, the net horizontal force created by this distribution is zero (Equation (4)), but the torque is not. Each friction force f can be written as

$f = \mu_s F_n$ and F_n is the normal force acting at the same point. The torque around the axis of the container created by this frictional force is $f \bar{r}_s$, where \bar{r}_s is the mean radius from the axis of the container to the finish (Figure 8). Summing torque from all contact points, the required T to start the liner sliding over the finish is

$$T = \mu_s \cdot F_v \cdot \bar{r}_s \quad (5)$$

Solving for μ_s yields:

$$\mu_s = \frac{T}{F_v \cdot \bar{r}_s} \quad (6)$$

Equation (6) shows that μ_s at the liner interface is the ratio of the torque required to initiate sliding to the product of the top load and the mean radius \bar{r}_s . Clearly, if we apply a known load F_v on the liner, and then increase the torque either clockwise or counterclockwise until sliding begins, the static coefficient of friction between liner and finish then can be determined. For instance, if a liner having a diameter of 28 mm ($\bar{r}_s = 0.45425$ in $\pm 18\%$) is loaded with $F_v = 1.32$ lb, and the torque required to start the liner sliding is 0.41 TIP $\pm 14\%$, the static coefficient of friction of the liner in contact with the finish is $0.69 \pm 32\%$.

The next step is to determine the static coefficient of friction between the threads of the closure and threads of the container, which is handled using a similar approach. The threads are assumed to be in continuous contact. A representative contact point is shown in Figure 9a where the closure thread contacts the container thread at some angle θ . The closure spins freely in Figure

9a because there is no contact between the liner and finish yet. The experiment was setup this way so that only thread-to-thread friction was involved. A free-body diagram of this system under clockwise torque looking along a radius is depicted in Figure 9b.

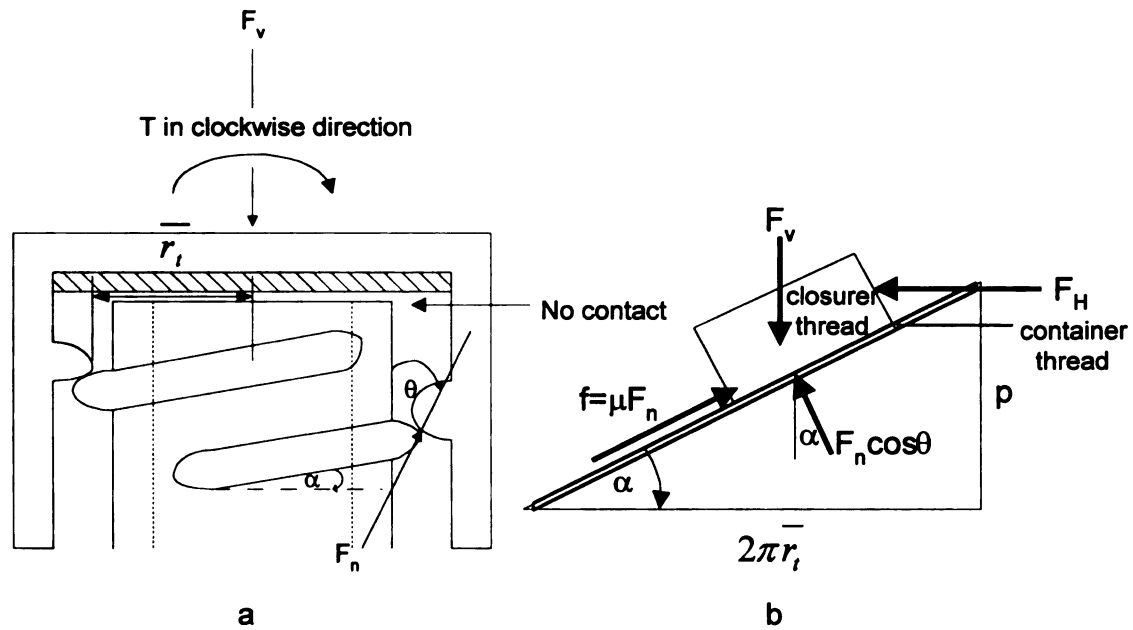


Figure 9 Free-Body Diagram of the Closure Thread and Container Thread in Contact

Solving the equilibrium equations yields the following:

$$\sum F_y = 0, \quad -F_v + F_n \cos \theta \cdot \cos \alpha + \mu_t \cdot F_n \cdot \sin \alpha = 0 \quad (7)$$

where μ_t is the static coefficient of friction at the thread interface, α is thread pitch angle, p is thread pitch, and θ is contact angle looking along the thread.

$$\text{So} \quad F_v = F_n \cdot (\cos \theta \cdot \cos \alpha + \mu_t \cdot \sin \alpha) \quad (8)$$

$$\sum F_x = 0, \quad \mu_t \cdot F_n \cdot \cos \alpha - F_n \cos \theta \cdot \sin \alpha - F_H = 0 \quad (9)$$

where F_H is the horizontal twisting force applied to the closure by the torque.

Rearranging Equation (9) gives:

$$F_H = F_n \cdot (\mu_t \cdot \cos \alpha - \cos \theta \cdot \sin \alpha) \quad (10)$$

Then the required torque to start clockwise twisting is

$$T = F_H \cdot \bar{r}_t \quad (11)$$

where \bar{r}_t is the mean radius at the point of contact.

Since F_n and F_H are known from Equations (8) and (10), Equation (11) can be written as

$$T = F_v \cdot \bar{r}_t \cdot \left(\frac{\mu_t \cos \alpha - \cos \theta \cdot \sin \alpha}{\cos \theta \cdot \cos \alpha + \mu_t \sin \alpha} \right) \quad (12)$$

The above equation can be related to the thread geometry by substituting for

$\sin \alpha$ and $\cos \alpha$ using the triangle shown in Figure 9b: $\sin \alpha = \frac{p}{l}$ and $\cos \alpha = \frac{2 \cdot \pi \cdot \bar{r}_t}{l}$,

where l is the length of a thread in one complete revolution and p is the vertical spacing between threads (thread pitch).

Then,

$$T = F_v \cdot \bar{r}_t \cdot \left(\frac{\mu_t \cdot 2 \cdot \pi \cdot \bar{r}_t - \cos \theta \cdot p}{\cos \theta \cdot 2 \cdot \pi \cdot \bar{r}_t + \mu_t p} \right) \quad (13)$$

Therefore, the static coefficient of friction between the thread of the closure and the thread of the container under clockwise twisting is

$$\mu_t = \frac{\cos \theta \cdot \bar{r}_t \cdot [T \cdot 2 \cdot \pi + F_v \cdot p]}{[\bar{r}_t^2 \cdot F_v \cdot 2 \cdot \pi - T \cdot p]} \quad (14)$$

The equation for determining the static coefficient of friction under counterclockwise twisting can be done in a similar manner except that the friction forces are reversed. The result is

$$\mu_t = \frac{\cos\theta \bar{r}_i [T \cdot 2\pi - F_v \cdot p]}{[\bar{r}_i^2 \cdot F_v \cdot 2\pi + T \cdot p]} \tag{15}$$

Equations (14) and (15) contain closure-container parameters (\bar{r}_i , θ , p) which are readily measured: only T and F_v are left to determine μ_t . Then if we apply a known load F_v and measure the torque T for starting a closure thread sliding on container thread either clockwise or counterclockwise, μ_t can be calculated. In addition, μ_t should be constant regardless of the twisting direction and the top load chosen.

To determine the static coefficient of friction between the thread of the closure and the thread of the container, the closure-container systems selected from Table 2, and 3 were based on the closure diameter, the types of mold, and color. The combinations are presented in Figure 10.

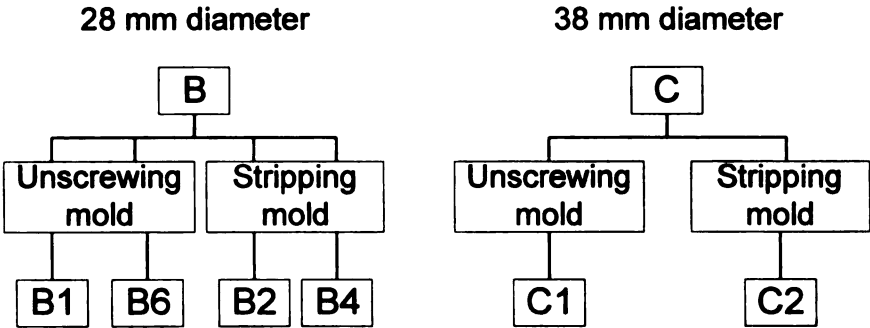


Figure 10 The Treatments Tested for the Static Coefficient of Friction at the Thread Interface

In this research, closures made from different types of mold will have different thread profiles as a result of different contact angle. The unscrewing mold of Figure 10 provides the “L” style thread profile. The threaded cores are unscrewed out of the closures so that precise thread dimensions can be made. In the stripping mold, the closures are stripped off the thread cores and have the “M” style thread profile. In Figure 10, there are 6 different treatments, with 5 runs for each treatment under clockwise and counterclockwise twisting. The series of the top loads used in each run range from 400 g to 2000 g with increments of 200 g. Equations (14) and (15) were used to calculate the static coefficient of friction.

The static coefficient of friction between the liner and the finish of the container was also obtained. The combinations of the treatments are shown in Figure 11, also with 5 runs for each treatment. The selection of the treatments was based on the closure diameter, the types of liner, and the method of attaching the liner to the inside of the closure.

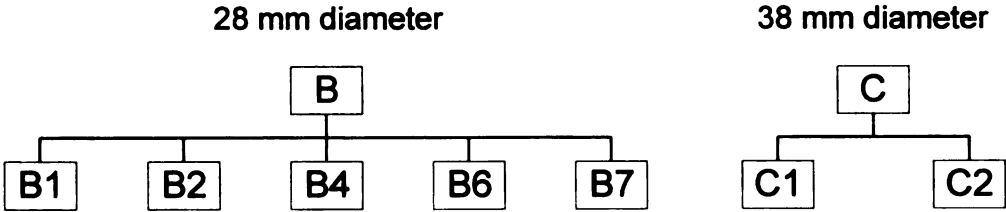


Figure 11 The Treatments Tested for the Static Coefficient of Friction at the Liner Interface

In order to achieve contact only between the liner and the finish of the container, all of the threads all around the neck of the container were eliminated using the grinding and hand sanding tools. Hence, the container was ready for testing in both twisting directions. The top loads used in this case were dependent on the closure diameter and liner type. The loads of 150 g, 200 g, 300 g, 400 g, 600 g, and 800 g were applied to closures containing the 28 mm diameter PE foam liner. Closures containing the 38 mm diameter PE foam liner were loaded with 200 g or 300 g, 400 g, 600 g, and 800 g. The 28 mm diameter paper pulp backing liners were subjected to a series of 600 g, 800 g, 1000 g, 1200 g and 1400 g. Equation (6) was used to calculate the static coefficient of friction at the liner interface.

3. Predictive model.

The application of mechanics to the closure-container system can be used to find the friction coefficients μ_s and μ_t separately when either application or removal torque takes place. In actual conditions, when the closure is applied on the container, both μ_s and μ_t are involved at the same time. The application torque imposed during application of a closure on the finish of a container is converted to compression of the liner against the finish-sealing surface. The conversion of torque to compression force at the sealing surface is not completely efficient because friction losses occur in the region of the seal as well as in contact area between closure threads and container threads. There are

two predictive models derived from the application of mechanics; an application torque model, and a removal torque model. Both models are developed by using an approach similar to that discussed in the coefficient of friction section. Free-body diagrams of the closure-container system under application and removal torque are shown in Figure 12. When the horizontal twisting force F_H is applied to the closure by the torque T , the magnitude of the applied torque T is composed of two parts: one from the liner interface and another from the thread interface. At the liner interface, the contribution to the torque is the same as Equation (5), which is repeated here as Equation (16) for reference in this section.

$$T = F_v \cdot \mu_s \cdot \bar{r}_s \quad (16)$$

Figure 12a shows that the closure thread is under the container thread at some contact angle θ which gives a result similar to Equation (13); the contribution to the application torque from thread-to-thread contact is

$$T = F_v \cdot \bar{r}_t \left[\frac{\cos \theta \cdot p + 2 \cdot \pi \cdot \mu_t \cdot \bar{r}_t}{\cos \theta \cdot 2 \cdot \pi \cdot \bar{r}_t - \mu_t \cdot p} \right] \quad (17)$$

Then Equations (16) and (17) are combined to give the total application torque

$$T = F_v \cdot \left[\bar{r}_t \left[\frac{\cos \theta \cdot p + 2 \cdot \pi \cdot \mu_t \cdot \bar{r}_t}{\cos \theta \cdot 2 \cdot \pi \cdot \bar{r}_t - \mu_t \cdot p} \right] + \mu_s \cdot \bar{r}_s \right] \quad (18)$$

where

T	= Application torque, (TIP)
F_v	= Sealing force, (lb)
p	= Thread pitch, (inches)

μ_t and μ_s = Coefficient of friction at thread interface,
and sealing surface

\bar{r}_t and \bar{r}_s = Mean radius of the thread contact,
and sealing surface, (inches)

θ = Contact angle, (degrees)

Equation (18) shows that the sealing force during application can also be calculated if the application torque is known. The removal torque is lower than the application torque for mechanical reasons. The predictive model for the removal torque is derived the same way as described above except that the F_H and friction forces are reversed as shown in Figures 12d and e. The result is

$$T' = F_v \left[\bar{r}_t \left[\frac{2\pi\mu_t\bar{r}_t - \cos\theta \cdot p}{\cos\theta \cdot 2\pi\bar{r}_t + \mu_t \cdot p} \right] + \mu_s \bar{r}_s \right] \quad (19)$$

Equations (18) and (19) are comparable to the McCarthy's equations. However, substantial differences occur in predicted torques using Equations (18) and (19) are expected due to the liner factor included.

Equation (19) shows that the removal torque is composed of two components. They are as follows:

$$F_v \bar{r}_t \left[\frac{2\pi\mu_t\bar{r}_t - \cos\theta \cdot p}{\cos\theta \cdot 2\pi\bar{r}_t + \mu_t \cdot p} \right] \text{ is the contribution produced by frictional restraint}$$

between the closure threads and container threads. This will be called the thread factor.

$F_v \mu_s \bar{r}_s$ is the contribution created by frictional restraint between the face of the liner and the container finish. This will be called the liner factor.

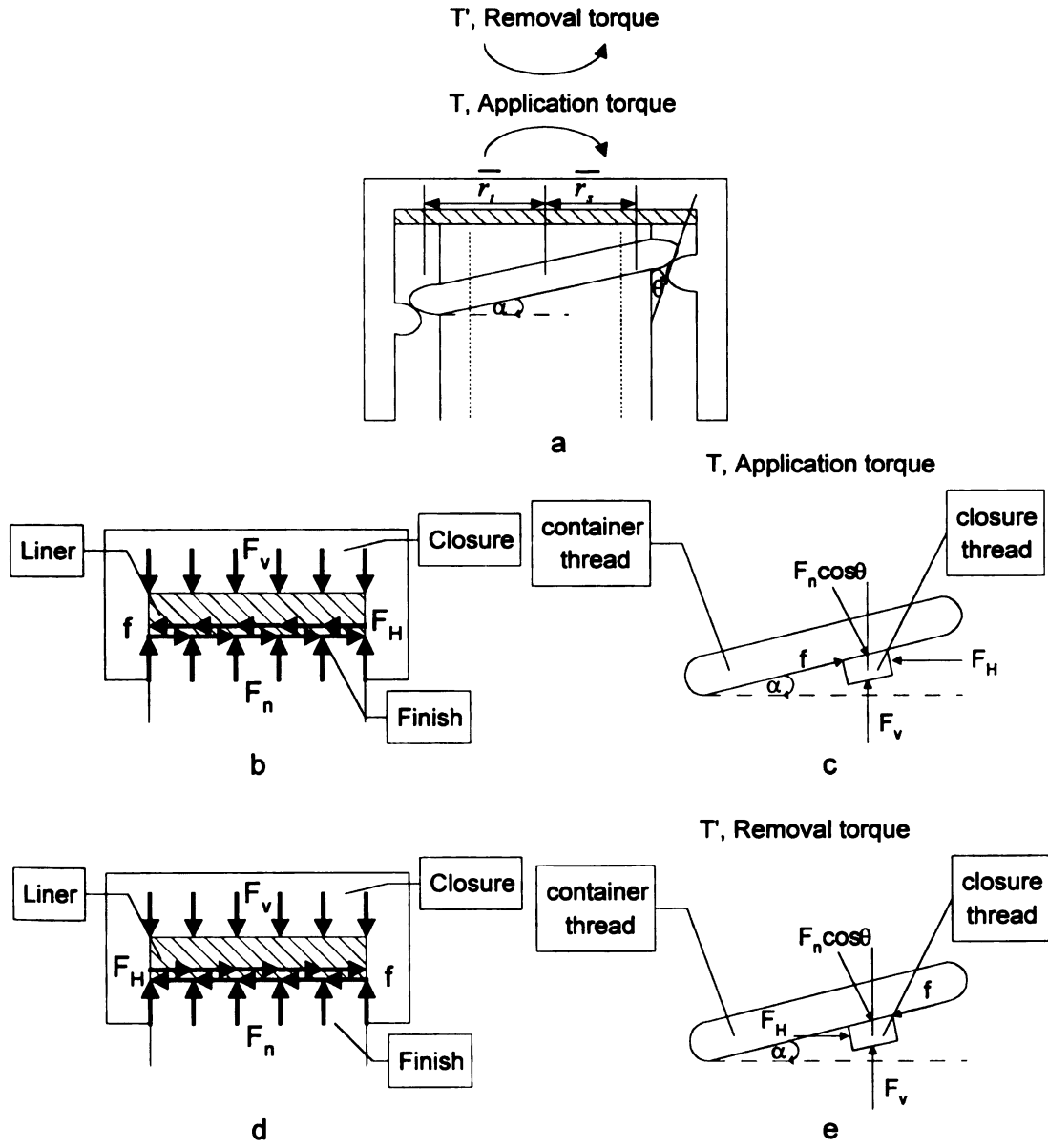


Figure 12 Free-Body Diagram of the Closure-Container System

If we use typical information of a 28-400 closure and a F-217 liner, then the magnitude of each factor can be computed separately. It will be found that the thread factor accounts for only 18% of total removal torque and the liner factor accounts for about 82% of total torque as shown in Figure 13.

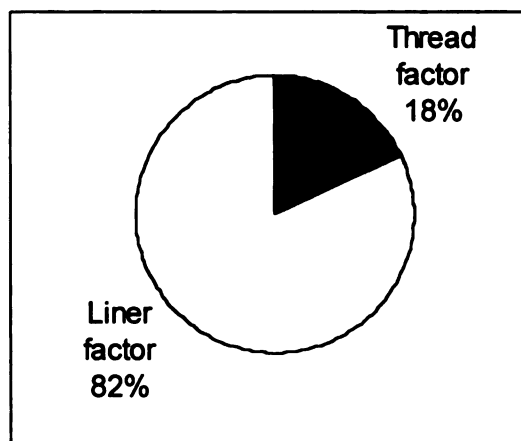


Figure 13. Relative Magnitude of Torque Contributed by Thread and Liner Factor

Figure 13 shows that the liner factor contributes much more to the removal torque than the threads do. Hence, the selection of the proper liner in relation to the container finish is very important in order to get the desired removal torque.

Thread factor determines whether or not the closure threads are self-locking. When a positive removal torque is obtained from the thread factor, the closure thread is said to be self-locking. Thus, the condition for self-locking is

$$2\pi\mu_t \bar{r}_t > \cos\theta.p \tag{20}$$

Solving for μ_t and relating the thread geometry to α gives

$$\mu_t > \cos\theta \tan\alpha \tag{21}$$

This relation states that self-locking is obtained whenever the coefficient of friction between closure threads and container threads is greater than the product of the tangent of the thread angle and the cosine of the contact angle. For example, the 28-400 closure-container system has a thread angle 2.96° and a contact angle $25.75^\circ \pm 19\%$, which means that in order to obtain self locking, a minimum static coefficient of friction at the thread interface of $0.047 \pm 19\%$ is needed to achieve this.

4. Sealing force

The sealing force is defined as the compression force at the sealing surface resulting from the translation of torque to the vertical force. This is F_v in the previous analysis. Currently, there is no easy way to measure this force directly in closure systems. This task is also interesting and challenging for investigators. The sealing force depends on the mechanical properties of the liner. At present, the specification of the tightness of closure-container systems is partly based on the removal torque. Equation (19) shows that if a certain similar removal torque is required on the different closure-container systems, they will have different sealing forces. The sealing force, F_v is what pushes the liner on the finish of the container. The removal torque is what needs to be applied to start the various surfaces sliding against friction forces. Therefore, the sealing force is a better indicator of the mechanical seal of the liner than the

removal torque. A low sealing force means that the compression force pushing the liner is low, so the mechanical seal protection is weak.

The mechanical characteristics of the liner significantly influence the sealing force. The most important of these properties in relation to the sealing force is viscoelasticity. Familiar examples of this behavior are present in many cases involving packaging materials. When foam cushions are used in a drop test, they do not completely return to their original initial thickness. Corrugated boxes also show similar behavior in a compression test. A box under compression will immediately relax if the test is momentarily stopped and never return to its original height after unloading. The concept to remember is that in viscoelastic materials, the force required to compress it is always more than the force required to restrain it during expansion.

A model consisting of a spring and a dashpot is useful in conceptualizing the viscoelastic behavior of the liner materials. The spring is considered an ideal solid element obeying Hooke's law and the dashpot is considered an ideal fluid element. The spring and dashpot can be connected in various ways to portray viscoelastic behavior. The particular combination of these elements used here is shown in Figure 14.

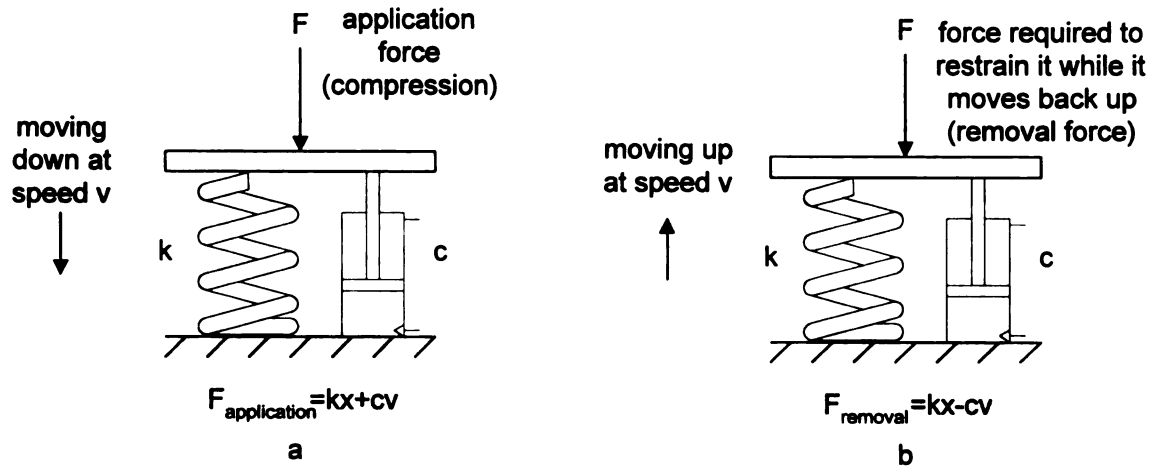


Figure 14 The Spring-Dashpot Concept for the Liner Materials under Compression

The force required to compress the liner and then restrain it during removal are expressed in Equations (22) and (23),

$$F_{\text{application}} = k.x + c.v \quad (22)$$

$$F_{\text{removal}} = k.x - c.v \quad (23)$$

where k is the spring constant, x is the amount of compression, c is the damping constant, and v is the compression rate.

At a particular compression x , the ratio of F_{removal} to $F_{\text{application}}$ is

$$\frac{F_{\text{removal}}}{F_{\text{application}}} = \frac{k.x - c.v}{k.x + c.v} < 1 \quad (24)$$

During compression, both the spring and dashpot push up and resist force $F_{\text{application}}$, but during expansion, the spring still pushes up while the dashpot pulls down. Basically, a dashpot acts to make the material want to stay in the shape

that it is in, while the spring acts to return it to its original shape. The magnitude of the damping and spring effect is dependent on c , and k respectively. If there is very little damping (low c as in metals), then the ratio of F_{removal} to $F_{\text{application}}$ is close to 1. At the opposite extreme, if there is a lot of damping (plastics, foams), the ratio is close to 0.

The above analogy says that the sealing force F_v in the predictive equations for the application torque is like the applied compression force F in Figure 14a, and F_v in the predictive equation for the removal torque is like the restraining force during removal in Figure 14b, which is smaller by some factor f ($0 < f < 1$). The “ f factor” in the spring-dashpot model depends on the size of “ c ” in relation to “ k ” and on how fast the closure is twisted during removal. This can be used to relate the F_v in both equations by using:

$$F_v \text{ in removal torque} = f \cdot F_v \text{ in application torque} \quad (25)$$

Substituting F_v from Equations (18) and (19) yields:

$$\left[\frac{T'}{k_r} \right] = f \cdot \left[\frac{T}{k_a} \right] \quad (26)$$

Rearranging Equation (26) gives:

$$f = \frac{k_a \cdot T'}{k_r \cdot T} \quad (27)$$

where $k_a = \left[\frac{-}{r_i} \left[\frac{2\pi \cdot \mu_i \cdot \bar{r}_i + \cos \theta \cdot p}{\cos \theta \cdot 2\pi r_i - \mu_i \cdot p} \right] + \mu_s \cdot \bar{r}_s \right]$ (inches)

$k_r = \left[\frac{-}{r_i} \left[\frac{2\pi \cdot \mu_i \cdot \bar{r}_i - \cos \theta \cdot p}{\cos \theta \cdot 2\pi r_i + \mu_i \cdot p} \right] + \mu_s \cdot \bar{r}_s \right]$ (inches)

T' = The measured removal torque (TIP)

T = The measured application torque (TIP)

The “f factor” is actually the ratio of the sealing force during removal to the sealing force during application so it is named “the sealing force ratio”. If the sealing force during application torque is equal to the sealing force during removal, then the liner is 100% efficient in holding the compression force. Consequently, the “f factor” or sealing force ratio can be used as the indicator to indicate how good the liner retains the sealing force. A low “f factor” means that the sealing force degrades too much. This indicator is very useful for the selection of the liner to achieve the desired removal torque.

The purpose of the predictive models was to evaluate these f factors. The models were used on all combinations of 28 and 38 mm diameter closure-liner system and five replicates of each combination were investigated. The Secure Pak torque tester electronic model calibrated according to ASTM D 3474-90, was used to measure the application and the removal torques. The procedure followed was essentially that outlined in ASTM D 3198-97: Standard Test Method for Application and Removal Torque of Threaded or Lug-Style Closures. The 28 and 38 mm diameter closures had a prescribed application torque of 14 TIP and 19 TIP respectively. There were two types of removal torque evaluated: the instantaneous removal torque, and the immediate removal torque. The instantaneous removal torque is when the samples are tested within 10 seconds after the closure is applied. The torque required to unscrew a closure 15 minutes after application is the immediate removal torque. The ratio of these two types of removal torque to the application torque was calculated and compared with the

theoretical ratio. Additionally, the “f factor” of each combination of closure and container also was calculated using Equation (27) and compared to the above ratio.

4. RESULTS

1. Cross-sectional measurement of the closure-container system

The casting treatments of 28 mm and 38 mm diameter shown in Figure 10 were applied with the prescribed application torque of 14 TIP and 19 TIP. They were measured the dimensions using the optical comparator. A summary of the data is shown in Table 4.

Table 4 Summary of the Dimension Parameters of Various Treatments Tested

Parameter	28 mm diameter				38 mm diameter	
	Unscrewing mold		Stripping mold		Unscrewing mold	Stripping mold
	B-B1	B-B6	B-B2	B-B4	C-C1	C-C2
T (inches)	1.0755	1.0755	1.0755	1.0755	1.4630	1.4630
E (inches)	0.9790	0.9790	0.9790	0.9790	1.3605	1.3605
I (inches)	0.8380	0.8380	0.8380	0.8380	1.2210	1.2210
p (inches)	0.167	0.167	0.167	0.167	0.167	0.167
angle α (degree)	2.96	2.96	2.96	2.96	2.16	2.16
\bar{r}_i	0.514	0.514	0.514	0.514	0.7059	0.7059
\bar{r}_s	0.45425	0.45425	0.45425	0.45425	0.64538	0.64538
angle θ (degree)	25.75	20	42.25	44.25	41.5	39.75

Note: The dimensions shown are to 4 decimal places because the optical comparator has this sensitivity, but the closures varied as follows;

T \pm 15%, E \pm 12%, I \pm 15%, \bar{r}_i \pm 24%, \bar{r}_s \pm 18%, angle θ \pm 19%

As indicated in Table 4, the effect of the types of the closure molds substantially shows on the contact angle θ of 28 mm diameter treatments. It was found that treatments made from the unscrewing mold had the contact angle θ about one half the value of those made from the stripping mold. This difference can be explained by the thread profiles: the "L" style and "M" style. The "L" style thread made on the unscrewing mold is the general purpose thread; it has the symmetrical threads with 30° pressure angle. The "M" or modified buttress thread found in the stripping mold has the angle of 45° from a line drawn perpendicular to the neck finish at the top, and 10° on the bottom. The examples of these thread profiles of the treatments tested are shown in Figure 15.

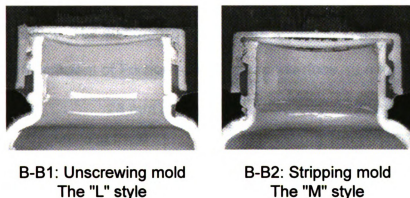


Figure 15 The "L" and "M" Thread Profiles Obtained from the Unscrewing and Stripping mold

Therefore, when each type of thread profile makes contact on the "M" style container thread, the systems have different contact angles. The 38 mm diameter treatments, however, show only small differences in the measured contact angle θ of these two types of molds. This is related to the amount of high

compression force generated during application. It is about 10-20 lb higher than that in the 28 mm diameter treatments. This amount of high compression force causing deformation occurred enough to stabilize the contact angle without further deformation even though they were tested on the different thread profiles.

Thus, the thread profiles strongly affect the contact angle of the 28 mm diameter closure-container systems but only slightly affect the 38 mm systems.

2. The static coefficient of friction measurement

A similar set of treatments tested in the former experiment was conducted by the TLRD method for measuring the static coefficient of friction at thread interface. The purpose of this test was to see what the static coefficient of friction values were in which they were measured directly from the closure-container in contact. The summarized results are shown in Table 5.

Table 5 Static Coefficient of Friction at the Thread Interface, μ_t , n = 5

	28 mm diameter				38 mm diameter	
	Unscrewing mold		Stripping mold		Unscrewing mold	Stripping mold
	B-B1 HDPE-PP white	B-B6 HDPE-PP black	B-B2 HDPE-PP white	B-B4 HDPE-PP black	C-C1 HDPE-PP white	C-C2 HDPE-PP white
Average	0.18	0.185	0.173	0.171	0.112	0.115
Standard deviation	0.018	0.021	0.017	0.016	0.014	0.013

Note: $\mu_t \pm 37\%$

The static coefficient of friction at the thread interface of all treatments shown in Table 5 is distributed within the narrow range from 0.171 to 0.185. There is no difference in μ_t between the white color treatments and the black color treatments in both types of mold. Comparing μ_t obtained from 28 mm diameter treatments and 38 mm diameter treatments, it shows that μ_t of the 38 mm system is slightly lower than the 28 mm system. The difference should come from the effect of manufacturing of closures, and the formula of materials used in processing closures. These factors can greatly affect on material properties of the closures. The standard deviation shows that the values obtained are repeatable, so it indicates that this method is consistent in measuring the static coefficient of friction at the thread interface.

The static coefficient of friction at the liner interface, μ_s is determined from the liner sliding against the finish of the HDPE container. The closures from various combinations of liners and methods of attaching the liner were tested by the TLRD method. The results are tabulated in the columns for each treatment in Table 6.

Table 6 Static Coefficient of Friction at the Liner Interface, μ_s , n = 5

	28 mm diameter					38 mm diameter	
	B-B1	B-B2	B-B4	B-B6	B-B7	C-C1	C-C2
Average	0.76	0.50	0.162	0.181	0.181	0.472	0.363
Standard deviation	0.124	0.073	0.027	0.030	0.030	0.085	0.073

Note: $\mu_s \pm 32\%$

B-B1: PE foam-HDPE, glued

B-B2: PE foam-HDPE, non-glued

B-B4: Paper pulp coated with Saran-HDPE, non-glued

B-B6: Paper pulp coated with polyvinyl lubricant film, glued

B-B7: Paper pulp coated with polyvinyl lubricant film, non-glued

C-C1: PE foam-HDPE, glued

C-C2: PE foam-HDPE, non-glued

The static coefficient of friction depends on not only the roughness of the material surface but also other material properties such as adhesion, compressive stress, and shear stress. This experiment shows the complexity of friction phenomena. The effect of different types of liner on the static coefficient of friction was determined in the 28 mm treatments. The measured results of 28 mm treatments shows that μ_s of the PE foam-HDPE is substantially higher than μ_s of the paper pulp coated-HDPE. The reason why the PE foam liner in contact with HDPE finish has more friction than the coated paper pulp is that the PE foam surface provides more adhesion in the contact area than the coated paper pulp liner does. In addition, the friction force f is required to overcome the adhesion in the contact area, A in the Equation (28). Then, the relationship can

state:

$$\mu_s = \frac{\text{Friction force}}{F_n} = \frac{A\tau}{A\sigma_y} = \frac{\tau}{\sigma_y} \quad (28)$$

where F_n is the sealing force F_v , σ_y is the compressive yield stress, and τ is the shear stress.

Clearly, the shear stress and the compressive yield stress are directly related to μ_s . Equation (28) is very useful to describe how the material properties of the liner materials influence the static coefficient of friction. In fact, the coated paper pulp liner is stiffer than the PE foam liner so its compressive yield stress should be higher than the compressive yield stress of the PE foam liner as a result of lower static coefficient of friction. The slip-stick characteristics also are considered as a factor causing high static coefficient of friction in the PE foam liner because these characteristics happen in most polymers when the test is conducted at low sliding speed. The next consideration on μ_s is the effect of different polymers coated on the paper pulp liner. The very thin film coating on the facing surface of the paper pulp liner, even though they are different kinds of polymers, showed only small differences within the set of liners (B-B4, B-B6, B-B7). It can be concluded that the paper pulp which functions as a backing material in the paper pulp liners is the most important effect in the static coefficient of friction at the liner interface.

The methods of attaching the liner to the inside of the closure are also interesting as to their effect on the static coefficient of friction. There are two attachment methods: glued, and non-glued. The closures made by both methods can be found in general products including in food and pharmaceutical products. The advantages of these methods regarding the effective seals are not clearly known yet. The experiment began to determine the static coefficient of friction of the non-glued treatments to use in the predictive models. The static coefficient of friction of the non-glued type is not the coefficient at the interface

between the liner and the finish but actually it is the coefficient of friction between the liner and the inside panel of the closure. The observation on the actual applications of closures either the PE foam liner or the coated paper pulp liners, which are attached by both methods, indicated that the static coefficient of friction of the non-glued type is not useful. When the removal torque was applied on the closures with the non-glued liners, it showed that the non-glued liners slide on the finish of the container following the removal direction. It means that in practical applications the static coefficient of friction between the liner and the finish of the container should be applied for the non-glued type rather than using the value deduced from the contact between the liner and the inside panel of the closure. Therefore, the coefficients of friction at the liner interface of the non-glued types (B-B2, B-B4, B-B7, C-C2) shown in Table 6 are not practicable to use in the predictive models. The values of the glued types made from the same material are applied in the models instead.

The measurement of the static coefficient of friction is dependent on the specific test conditions and configurations. The TLRD method is based on the practical situations when the closure is applied on the container. Thus, it is considered an appropriate method for determining the static coefficient of friction at the thread interface and at the liner interface.

3. The predictive model

All 8 systems of the 28mm diameter and 2 systems of 38 mm diameter shown in Table 3 were used to evaluate the predictive models (Equation (17), (18)) and the “f factor” (Equation (27)) respectively. The measured results from

Table 4 were used to calculate the theoretical ratio of the removal torque, T' to the application torque, T . As discussed in Chapter 2, the models do not completely represent the actual closure-container system under the torque because the relaxation factor is not incorporated in the models. Thus, the predictive model for the removal torque is supposed to overestimate. To get a better picture, the predicted removal, T' is then calculated using the measured application torque, AT and the data needed from Table 4 and compared with the measured instantaneous removal torque (ISRT), and the measured immediate removal torque (IRT)) as shown in Table 7.

Table 7 Comparison of the Predicted Removal Torque, T' and the Measured Removal Torque, ISRT, and IRT

Treatment	Instantaneous removal (10 sec)			Immediate removal (15 min)		
	AT (TIP)	ISRT (TIP)	T' (TIP)	AT (TIP)	IRT (TIP)	T' (TIP)
B-B1	13.84	6.60	12.23	13.96	6.36	12.34
B-B2	14.08	11.16	12.48	14.16	9.28	12.55
B-B3	14.18	10.60	12.57	14.04	9.02	12.45
B-B4	14.10	11.22	10.57	14.10	8.46	10.57
B-B5	14.08	12.80	10.56	13.92	8.98	10.44
B-B6	14.14	9.76	10.44	14.02	8.66	10.36
B-B7	14.14	12.74	10.74	13.88	9.72	10.54
B-B8	14.08	11.46	10.69	13.96	9.88	10.60
C-C1	19.30	12.24	16.90	19.10	9.14	16.72
C-C2	18.94	16.28	16.13	19.26	12.96	16.40

Note: AT, ISRT and IRT \pm 4%, T' \pm 26%

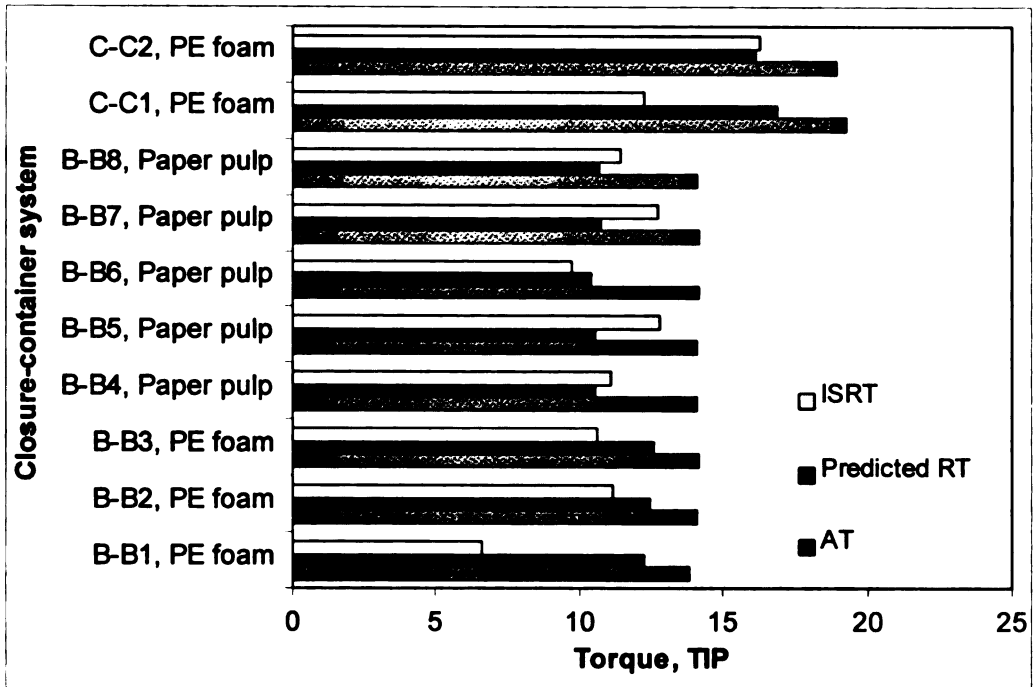


Figure 16 Comparison of ISRT and T'

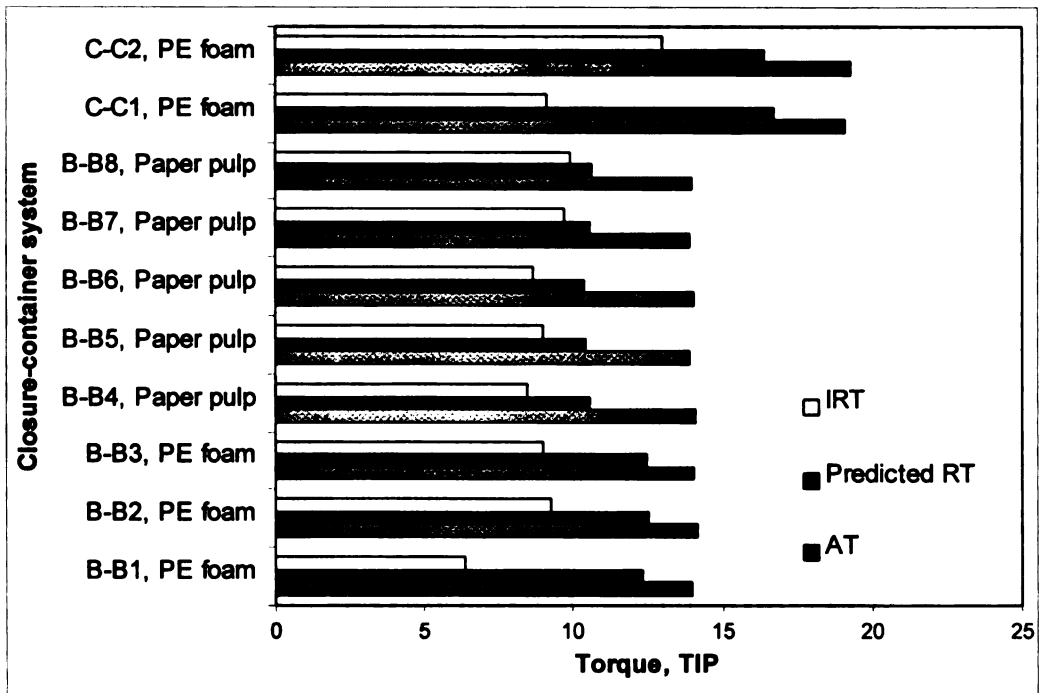


Figure 17 Comparison of IRT and T'

Generally, the instantaneous removal torque, ISRT is not useful for the practical applications because the measured torque at this period (within 10 sec) is not stable so the immediate removal torque, IRT (15 min) is the standard measurement. However, this comparison is intended to illustrate the effect of relaxation behavior of the closure-container system. As shown in Table 7, the removal torque decreases over time after application to 10 sec (ISRT) and 15 min (IRT). The effect of relaxation behavior especially from the liner materials largely affects the removal torque obtained. In Figure 16, the random behavior of ISRT could be noticed because the relaxation is not complete within 10 seconds. In general, relaxation occurs in a closure-container system because the liner has been loaded past its yield point and will creep and flow to get out from the excessive load. Figure 17 depicts that the predicted removal torque, T' of all treatments tested is overestimated by 12% to 94% the measured value to be expected. The wide range of overestimation was due to the different relaxation behavior of liner materials.

To quantitatively evaluate the performance of the predictive models, the theoretical ratio between T' to T was calculated to compare with the measured ratios ISRT to AT and IRT to AT. In addition, the “f factor” or the sealing force ratio of each treatment was also calculated and compared to the above ratios in Table 8 and 9. The theoretical ratio (T'/T) is based on the rigid body concept so theoretically it should be close to the measured ratio (ISRT/AT) which is measured within 10 sec after application. However, Table 8 shows that it deviated about -0.16 to $+0.40$ from the measured ratio. This reveals that

relaxation takes place as soon as the application torque is done. The theoretical ratio was an overestimation for the PE foam liner but an underestimation in the coated paper pulp liners. So it means that the relaxation in the PE foam liner occurred faster than the coated paper pulp liner. The relationship between the removal torque and the application torque is well described by comparing the ratio. For example, treatment B-B1: PE foam liner having the ratio of ISRT/RT of 0.48 means if the closure is applied with 10 TIP, the instantaneous removal torque of 4.8 TIP will be obtained. In other words, the efficiency of transferring from AT to ISRT is only 48%. Clearly understanding the interpretation of the ratio is necessary because it indicates the enormous effect of the stress relaxation on the removal torque. The measured ratios in Tables 8 and 9 of glued liner treatments (B-B1, B-B6, C-C1) show interesting results. These treatments have lower measured ratio than non-glued liner treatments which have the same liner material. This could be the result of the glued liner. When the closure is applied, the friction forces at the liner interface are developed. One face of the liner is glued on the inside panel of the closure which does not allow the liner to move. It is like two faces of the liner are fixed and when moved by the twisting force; the sheer stress of the liner itself is then simultaneously produced, along with the compression, which results in creating the wrinkles on the liner surface. The friction forces at the liner interface will decrease drastically and cause the lower removal torque. The comparison made on the ratio of the immediate removal torque to the application torque (IRT/AT) in Table 9 also shows similar results; the theoretical ratio was overestimated in all treatments. This is different from

the ratio of ISRT/AT in Table 8 because during instantaneous removal torque, the relaxation is just beginning so is not complete yet, and the liner materials react in the relaxation differently. Subsequently, this finding suggests that more work is needed to refine the predictive models.

Table 8 Comparison of T'/T and ISRT/AT, and the "f factor" or sealing force ratio

Treatment	Liner system	T'/T	ISRT/AT	"f factor"
B-B1	PE foam, glued	0.88	0.48	0.54
B-B2	PE foam, non-glued	0.89	0.79	0.89
B-B3	PE foam, non-glued	0.89	0.75	0.84
B-B4	P/SF, non-glued	0.75	0.80	1.06
B-B5	P/SF, non-glued	0.75	0.91	1.21
B-B6	P/RVTLF, glued	0.74	0.69	0.94
B-B7	P/RVTLF, non-glued	0.76	0.90	1.19
B-B8	P/RVTLF, non-glued	0.76	0.81	1.07
C-C1	PE foam, glued	0.88	0.63	0.72
C-C2	PE foam, non-glued	0.85	0.86	1.01

Note: T'/T \pm 17%, ISRT/AT \pm 8%, the "f factor" or sealing force ratio \pm 29%

Table 9 Comparison of T'/T and IRT/AT, and the "f factor" or sealing force ratio

Treatment	Liner system	T'/T	IRT/AT	"f factor"
B-B1	PE foam, glued	0.88	0.46	0.52
B-B2	PE foam, non-glued	0.89	0.66	0.74
B-B3	PE foam, non-glued	0.89	0.64	0.72
B-B4	P/SF, non-glued	0.75	0.60	0.80
B-B5	P/SF, non-glued	0.75	0.65	0.86
B-B6	P/RVTLF, glued	0.74	0.62	0.84

Table 9 (cont'd)

B-B7	P/RVTLF, non-glued	0.76	0.70	0.92
B-B8	P/RVTLF, non-glued	0.76	0.71	0.93
C-C1	PE foam, glued	0.88	0.48	0.55
C-C2	PE foam, non-glued	0.85	0.67	0.79

Note: T'/T ± 17%, IRT/AT ± 8%, the “f factor” or sealing force ratio ± 25%

The “f factor” or the sealing force ratio which indicates the capability of the liner to maintain the sealing force is shown in Tables 8 and 9. The “f factor” is a better indicator than using the measured ratio RT to AT to determine the effectiveness of the liner. Table 8 shows that some treatments had the “f factor” or sealing force ratio more than 1, this is due to the compound error introduced by the measuring devices ($\pm 25\%$). The “f factor” represents the efficiency of the liner in holding the sealing force, whereas the measured ratio portrays the efficiency in changing the application torque to the removal torque. The following example will show the justification of a good liner using the “f factor”. The comparison between treatment B-B2 and B-B6 in Table 9 says that treatment B-B6 is poorer than treatment B-B2 if using the measured ratio IRT/AT; however, the “f factor” indicates that treatment B-B6 is a better liner because it can hold the sealing force 10% more than what B-B2 does when applied for 15 min. The “f factor” shown in Figure 18 when closure is applied for 10 sec and 15 min indicates that it changes over time. One interesting application of this factor as a function of time is using it to show the decay rate of the sealing force ratio over time. So the selection of liner can be reasonably made from the results in order

to meet the desired removal torque at a certain time. Figure 17 suggests that the coated paper pulp liners retain the sealing force after 15 min application better than the PE foam liner. This retention is the result of the fact that the compressive yield stress of the coated paper pulp liners is higher than compressive yield stress of the PE foam liner and so it will impede the stress relaxation more than will PE foam. Consequently, the sealing force of the coated paper pulp liners after application is higher than the PE foam liner.

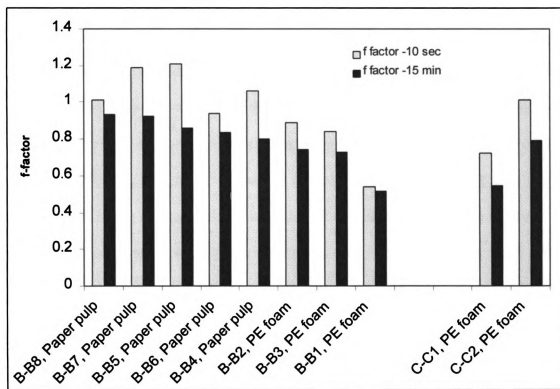


Figure 18 Comparison of the “f factor” 10 sec and 15 min after Application

Even though the results from the predictive model of the removal torque are an overestimation, the predictive model is still useful because the sealing

force during removal can be calculated by this equation. By determining the ratio of the sealing force during removal to the sealing force during application, the “f factor” or the sealing force ratio is obtained. The “f factor” can assist in the selection of the proper liner for the effective sealing from the interpretation previously described.

5. CONCLUSIONS

The TLRD method utilizing the static equilibrium approach was developed to determine the static coefficient of friction at the thread interface and at the liner interface. This method was validated under various experimental conditions and gave acceptable results. The concept of this method is simple and works well in directly measuring the static coefficient of friction under the practical conditions where the closure and the container are in contact. The static coefficient of friction is an important piece of information for the development of the predictive model.

The present predictive model does not fully describe the closure-container system since it does not account for the viscoelastic properties and the function of time. Much work remains to improve the accuracy of predicted results and to make the model more realistic. However, it is still useful in calculating the sealing force during removal which is proposed in this research. The sealing force is a better indicator than the removal torque in determining how good is the seal.

The liner is the most important factor in contribution to the removal torque. The spring-dashpot model well describes the liner material behavior under compression. The “f factor” or sealing force ratio deduced from the damping and spring effect in the liner is an essential indicator for determining how good the liner retains the sealing force. The application of the “f factor” shows that the paper pulp liner provides better retention of the sealing force than the PE foam liner after application for 15 min. These results might contradict current belief

and practice, but they seem to be valid. The closure-container system thus functions through the interaction of many material properties including the static coefficient of friction, the liner, and other characteristics of threaded closure.

Many interesting issues have been found during this research. Future researches should be conducted to compare the use of the removal torque and the sealing force as the indicator for the mechanical seal of the closure-container system. The effects of different thread profiles and geometry of the closure-container system on the mechanical seal also need to be investigated because they are generally present in practical applications. In addition, there are only a few published studies about the characteristics of the liner materials. This area should be scrutinized; especially the mechanical properties of the liner materials as these affect the mechanical seal of the closure-container system.

APPENDIX

Table 10 Raw Data of the Static Coefficient of Friction at the Thread Interface

B-B1	contact ang	25.75	degree			
	r _t =	0.514	in	T=1.0755	E= 0.9790	
	p=	0.167	in	(1 in/6 thrd)		
	d=	4.048	in			
Run 1	CW	28 mm	White			
	F _v , g	F _v , lb	F, g	F, lb	T, in-lb	μ _{cw}
	400	0.88	6.16	0.01	0.05	0.16
	600	1.32	9.16	0.02	0.08	0.16
	800	1.76	13.16	0.03	0.12	0.16
	1000	2.21	14.66	0.03	0.13	0.15
	1200	2.65	18.66	0.04	0.17	0.16
	1400	3.09	21.16	0.05	0.19	0.15
	1600	3.53	24.66	0.05	0.22	0.16
	1800	3.97	28.56	0.06	0.25	0.16
	2000	4.41	30.16	0.07	0.27	0.15
					Avg	0.16
					Sd(n-1)	0.004
					n	9

B-B1	contact ang	25.75	degree			
	r _t =	0.514	in	T=1.0755	E= 0.9790	
	p=	0.167	in	(1 in/6 thrd)		
	d=	4.048	in			
Run 1	CCW	28 mm	White			
	F _v , g	F _v , lb	F, g	F, lb	T, in-lb	μ _{ccw}
	400	0.88	12.16	0.03	0.11	0.17
	600	1.32	18.16	0.04	0.16	0.17
	800	1.76	24.16	0.05	0.22	0.17
	1000	2.21	32.16	0.07	0.29	0.18
	1200	2.65	39.16	0.09	0.35	0.18
	1400	3.09	44.16	0.10	0.39	0.17
	1600	3.53	48.16	0.11	0.43	0.16
	1800	3.97	50.16	0.11	0.45	0.15
	2000	4.41	55.66	0.12	0.50	0.15
					Avg	0.17
					Sd(n-1)	0.012
					n	9

Table 10 (cont'd)

B-B1	contact ang	25.75	degree			
	r_t =	0.514	in	T=1.0755	E= 0.9790	
	p=	0.167	in	(1 in/6 thrd)		
	d=	4.048	in			
Run 2	CW	28 mm	White			
	F_v , g	F_v , lb	F, g	F, lb	T, in-lb	μ_{cw}
	400	0.88	8.16	0.02	0.07	0.19
	600	1.32	11.66	0.03	0.10	0.19
	800	1.76	15.16	0.03	0.14	0.18
	1000	2.21	19.16	0.04	0.17	0.18
	1200	2.65	22.66	0.05	0.20	0.18
	1400	3.09	25.16	0.06	0.22	0.18
	1600	3.53	27.16	0.06	0.24	0.17
	1800	3.97	30.66	0.07	0.27	0.17
	2000	4.41	34.16	0.08	0.30	0.17
					Avg	0.18
					Sd(n-1)	0.009
					n	9

B-B1	contact ang	25.75	degree			
	r_t =	0.514	in	T=1.0755	E= 0.9790	
	p=	0.167	in	(1 in/6 thrd)		
	d=	4.048	in			
Run 2	CCW	28 mm	White			
	F_v , g	F_v , lb	F, g	F, lb	T, in-lb	μ_{ccw}
	400	0.88	16.16	0.04	0.14	0.24
	600	1.32	22.16	0.05	0.20	0.21
	800	1.76	30.16	0.07	0.27	0.22
	1000	2.21	35.16	0.08	0.31	0.20
	1200	2.65	41.66	0.09	0.37	0.20
	1400	3.09	49.16	0.11	0.44	0.20
	1600	3.53	53.16	0.12	0.47	0.19
	1800	3.97	41.16	0.09	0.37	0.11
	2000	4.41	68.16	0.15	0.61	0.19
					Avg	0.20
					Sd(n-1)	0.034
					n	9

Table 10 (cont'd)

B-B1	contact ang	25.75	degree			
	r_t =	0.514	in	T=1.0755	E= 0.9790	
	p=	0.167	in	(1 in/6 thrd)		
	d=	4.048	in			
Run 3	CW	28 mm	White			
	F_v, g	F_v, lb	F, g	F, lb	T, in-lb	μ_{cw}
	400	0.88	8.66	0.02	0.08	0.20
	600	1.32	12.16	0.03	0.11	0.19
	800	1.76	16.16	0.04	0.14	0.19
	1000	2.21	19.16	0.04	0.17	0.18
	1200	2.65	23.16	0.05	0.21	0.18
	1400	3.09	25.16	0.06	0.22	0.18
	1600	3.53	27.66	0.06	0.25	0.17
	1800	3.97	30.16	0.07	0.27	0.17
	2000	4.41	35.16	0.08	0.31	0.17
					Avg	0.18
					Sd(n-1)	0.012
					n	9

B-B1	contact ang	25.75	degree			
	r_t =	0.514	in	T=1.0755	E= 0.9790	
	p=	0.167	in	(1 in/6 thrd)		
	d=	4.048	in			
Run 3	CCW	28 mm	White			
	F_v, g	F_v, lb	F, g	F, lb	T, in-lb	μ_{ccw}
	400	0.88	15.16	0.03	0.14	0.22
	600	1.32	21.16	0.05	0.19	0.20
	800	1.76	26.16	0.06	0.23	0.18
	1000	2.21	32.16	0.07	0.29	0.18
	1200	2.65	38.16	0.08	0.34	0.18
	1400	3.09	43.16	0.10	0.39	0.17
	1600	3.53	49.66	0.11	0.44	0.17
	1800	3.97	58.16	0.13	0.52	0.18
	2000	4.41	64.66	0.14	0.58	0.18
					Avg	0.18
					Sd(n-1)	0.016
					n	9

Table 10 (cont'd)

B-B1	contact ang	25.75	degree			
	r_t =	0.514	in	T=1.0755	E= 0.9790	
	p=	0.167	in	(1 in/6 thrd)		
	d=	4.048	in			
Run 4	CW	28 mm	White			
	F_v , g	F_v , lb	F, g	F, lb	T, in-lb	μ_{cw}
	400	0.88	8.66	0.02	0.08	0.20
	600	1.32	12.16	0.03	0.11	0.19
	800	1.76	16.16	0.04	0.14	0.19
	1000	2.21	19.16	0.04	0.17	0.18
	1200	2.65	23.16	0.05	0.21	0.18
	1400	3.09	26.16	0.06	0.23	0.18
	1600	3.53	30.66	0.07	0.27	0.18
	1800	3.97	34.16	0.08	0.30	0.18
	2000	4.41	39.16	0.09	0.35	0.19
					Avg	0.19
					Sd(n-1)	0.007
					n	9

B-B1	contact ang	25.75	degree			
	r_t =	0.514	in	T=1.0755	E= 0.9790	
	p=	0.167	in	(1 in/6 thrd)		
	d=	4.048	in			
Run 4	CCW	28 mm	White			
	F_v , g	F_v , lb	F, g	F, lb	T, in-lb	μ_{ccw}
	400	0.88	14.66	0.03	0.13	0.21
	600	1.32	20.16	0.04	0.18	0.19
	800	1.76	25.16	0.06	0.22	0.17
	1000	2.21	31.16	0.07	0.28	0.17
	1200	2.65	36.16	0.08	0.32	0.17
	1400	3.09	41.66	0.09	0.37	0.16
	1600	3.53	48.16	0.11	0.43	0.16
	1800	3.97	53.66	0.12	0.48	0.16
	2000	4.41	61.16	0.13	0.55	0.17
					Avg	0.17
					Sd(n-1)	0.016
					n	9

Table 10 (cont'd)

B-B1	contact ang	25.75	degree			
	r _t =	0.514	in	T=1.0755	E= 0.9790	
	p=	0.167	in	(1 in/6 thrd)		
	d=	4.048	in			
Run 5	CW	28 mm	White			
	F _v , g	F _v , lb	F, g	F, lb	T, in-lb	μ _{cw}
	400	0.88	8.66	0.02	0.08	0.20
	600	1.32	12.66	0.03	0.11	0.20
	800	1.76	16.16	0.04	0.14	0.19
	1000	2.21	19.66	0.04	0.18	0.19
	1200	2.65	23.16	0.05	0.21	0.18
	1400	3.09	26.16	0.06	0.23	0.18
	1600	3.53	30.16	0.07	0.27	0.18
	1800	3.97	34.16	0.08	0.30	0.18
	2000	4.41	37.16	0.08	0.33	0.18
					Avg	0.19
					Sd(n-1)	0.008
					n	9

B-B1	contact ang	25.75	degree			
	r _t =	0.514	in	T=1.0755	E= 0.9790	
	p=	0.167	in	(1 in/6 thrd)		
	d=	4.048	in			
Run 5	CCW	28 mm	White			
	F _v , g	F _v , lb	F, g	F, lb	T, in-lb	μ _{ccw}
	400	0.88	14.16	0.03	0.13	0.20
	600	1.32	20.66	0.05	0.18	0.19
	800	1.76	26.16	0.06	0.23	0.18
	1000	2.21	32.16	0.07	0.29	0.18
	1200	2.65	38.16	0.08	0.34	0.18
	1400	3.09	43.66	0.10	0.39	0.17
	1600	3.53	49.16	0.11	0.44	0.17
	1800	3.97	56.16	0.12	0.50	0.17
	2000	4.41	62.16	0.14	0.55	0.17
					Avg	0.18
					Sd(n-1)	0.011
					n	9

Table 10 (cont'd)

B-B2	contact ang	42.25	degree			
	r_t =	0.514	in	T=1.0755	E= 0.9790	
	p=	0.167	in	(1 in/6 thrd)		
	d=	4.048	in			
Run 1	CW	28 mm	White			
	F_v , g	F_v , lb	F, g	F, lb	T, in-lb	μ_{cw}
	400	0.88	10.16	0.02	0.09	0.19
	600	1.32	12.16	0.03	0.11	0.16
	800	1.76	17.16	0.04	0.15	0.16
	1000	2.21	24.66	0.05	0.22	0.18
	1200	2.65	22.66	0.05	0.20	0.15
	1400	3.09	29.16	0.06	0.26	0.16
	1600	3.53	33.66	0.07	0.30	0.16
	1800	3.97	35.16	0.08	0.31	0.15
	2000	4.41	47.66	0.11	0.43	0.18
					Avg	0.17
					Sd(n-1)	0.014
					n	9

B-B2	contact ang	42.25	degree			
	r_t =	0.514	in	T=1.0755	E= 0.9790	
	p=	0.167	in	(1 in/6 thrd)		
	d=	4.048	in			
Run 1	CCW	28 mm	White			
	F_v , g	F_v , lb	F, g	F, lb	T, in-lb	μ_{ccw}
	400	0.88	13.66	0.03	0.12	0.16
	600	1.32	19.16	0.04	0.17	0.15
	800	1.76	29.66	0.07	0.26	0.18
	1000	2.21	35.16	0.08	0.31	0.16
	1200	2.65	42.66	0.09	0.38	0.17
	1400	3.09	56.17	0.12	0.50	0.19
	1600	3.53	60.66	0.13	0.54	0.18
	1800	3.97	66.66	0.15	0.59	0.17
	2000	4.41	77.16	0.17	0.69	0.18
					Avg	0.17
					Sd(n-1)	0.014
					n	9

Table 10 (cont'd)

B-B2	contact ang	42.25	degree			
	r_t =	0.514	in	T=1.0755	E= 0.9790	
	p=	0.167	in	(1 in/6 thrd)		
	d=	4.048	in			
Run 2	CW	28 mm	White			
	F_v , g	F_v , lb	F, g	F, lb	T, in-lb	μ_{cw}
	400	0.88	11.16	0.02	0.10	0.20
	600	1.32	13.16	0.03	0.12	0.17
	800	1.76	12.66	0.03	0.11	0.13
	1000	2.21	21.66	0.05	0.19	0.17
	1200	2.65	23.16	0.05	0.21	0.15
	1400	3.09	27.16	0.06	0.24	0.15
	1600	3.53	35.16	0.08	0.31	0.17
	1800	3.97	43.66	0.10	0.39	0.18
	2000	4.41	55.16	0.12	0.49	0.20
					Avg	0.17
					Sd(n-1)	0.023
					n	9

B-B2	contact ang	42.25	degree			
	r_t =	0.514	in	T=1.0755	E= 0.9790	
	p=	0.167	in	(1 in/6 thrd)		
	d=	4.048	in			
Run 2	CCW	28 mm	White			
	F_v , g	F_v , lb	F, g	F, lb	T, in-lb	μ_{ccw}
	400	0.88	16.16	0.04	0.14	0.19
	600	1.32	21.16	0.05	0.19	0.16
	800	1.76	24.66	0.05	0.22	0.14
	1000	2.21	41.66	0.09	0.37	0.20
	1200	2.65	38.16	0.08	0.34	0.15
	1400	3.09	53.16	0.12	0.47	0.18
	1600	3.53	59.66	0.13	0.53	0.18
	1800	3.97	63.16	0.14	0.56	0.16
	2000	4.41	78.66	0.17	0.70	0.19
					Avg	0.17
					Sd(n-1)	0.021
					n	9

Table 10 (cont'd)

B-B2	contact ang	42.25	degree			
	r_t =	0.514	in	T=1.0755	E= 0.9790	
	p=	0.167	in	(1 in/6 thrd)		
	d=	4.048	in			
Run 3	CW	28 mm	White			
	F_v , g	F_v , lb	F, g	F, lb	T, in-lb	μ_{cw}
	400	0.88	10.66	0.02	0.10	0.20
	600	1.32	14.66	0.03	0.13	0.18
	800	1.76	19.16	0.04	0.17	0.18
	1000	2.21	22.66	0.05	0.20	0.17
	1200	2.65	22.16	0.05	0.20	0.15
	1400	3.09	32.66	0.07	0.29	0.18
	1600	3.53	35.16	0.08	0.31	0.17
	1800	3.97	36.66	0.08	0.33	0.16
	2000	4.41	46.66	0.10	0.42	0.18
					Avg	0.17
					Sd(n-1)	0.014
					n	9

B-B2	contact ang	42.25	degree			
	r_t =	0.514	in	T=1.0755	E= 0.9790	
	p=	0.167	in	(1 in/6 thrd)		
	d=	4.048	in			
Run 3	CCW	28 mm	White			
	F_v , g	F_v , lb	F, g	F, lb	T, in-lb	μ_{ccw}
	400	0.88	16.66	0.04	0.15	0.20
	600	1.32	25.16	0.06	0.22	0.20
	800	1.76	28.16	0.06	0.25	0.16
	1000	2.21	37.66	0.08	0.34	0.18
	1200	2.65	41.66	0.09	0.37	0.16
	1400	3.09	48.66	0.11	0.43	0.16
	1600	3.53	59.66	0.13	0.53	0.18
	1800	3.97	62.66	0.14	0.56	0.16
	2000	4.41	80.66	0.18	0.72	0.19
					Avg	0.18
					Sd(n-1)	0.017
					n	9

Table 10 (cont'd)

B-B2	contact ang	42.25	degree			
	r_t =	0.514	in	T=1.0755	E= 0.9790	
	p=	0.167	in	(1 in/6 thrd)		
	d=	4.048	in			
Run 4	CW	28 mm	White			
	F_v , g	F_v , lb	F, g	F, lb	T, in-lb	μ_{cw}
	400	0.88	11.16	0.02	0.10	0.20
	600	1.32	10.66	0.02	0.10	0.14
	800	1.76	18.16	0.04	0.16	0.17
	1000	2.21	20.16	0.04	0.18	0.16
	1200	2.65	25.16	0.06	0.22	0.16
	1400	3.09	29.16	0.06	0.26	0.16
	1600	3.53	36.16	0.08	0.32	0.17
	1800	3.97	38.66	0.09	0.35	0.16
	2000	4.41	44.66	0.10	0.40	0.17
					Avg	0.17
					Sd(n-1)	0.016
					n	9

B-B2	contact ang	42.25	degree			
	r_t =	0.514	in	T=1.0755	E= 0.9790	
	p=	0.167	in	(1 in/6 thrd)		
	d=	4.048	in			
Run 4	CCW	28 mm	White			
	F_v , g	F_v , lb	F, g	F, lb	T, in-lb	μ_{ccw}
	400	0.88	16.66	0.04	0.15	0.20
	600	1.32	25.16	0.06	0.22	0.20
	800	1.76	28.16	0.06	0.25	0.16
	1000	2.21	37.66	0.08	0.34	0.18
	1200	2.65	41.66	0.09	0.37	0.16
	1400	3.09	48.66	0.11	0.43	0.16
	1600	3.53	59.66	0.13	0.53	0.18
	1800	3.97	62.66	0.14	0.56	0.16
	2000	4.41	80.66	0.18	0.72	0.19
					Avg	0.18
					Sd(n-1)	0.017
					n	9

Table 10 (cont'd)

B-B2	contact ang	42.25	degree			
	r_t =	0.514	in	T=1.0755	E= 0.9790	
	p=	0.167	in	(1 in/6 thrd)		
	d=	4.048	in			
Run 5	CW	28 mm	White			
	F_v , g	F_v , lb	F, g	F, lb	T, in-lb	μ_{cw}
	400	0.88	9.66	0.02	0.09	0.18
	600	1.32	11.16	0.02	0.10	0.15
	800	1.76	21.66	0.05	0.19	0.20
	1000	2.21	23.16	0.05	0.21	0.17
	1200	2.65	26.66	0.06	0.24	0.17
	1400	3.09	27.66	0.06	0.25	0.15
	1600	3.53	39.66	0.09	0.35	0.18
	1800	3.97	39.66	0.09	0.35	0.17
	2000	4.41	44.66	0.10	0.40	0.17
					Avg	0.17
					Sd(n-1)	0.015
					n	9

B-B2	contact ang	42.25	degree			
	r_t =	0.514	in	T=1.0755	E= 0.9790	
	p=	0.167	in	(1 in/6 thrd)		
	d=	4.048	in			
Run 5	CCW	28 mm	White			
	F_v , g	F_v , lb	F, g	F, lb	T, in-lb	μ_{ccw}
	400	0.88	14.66	0.03	0.13	0.17
	600	1.32	20.66	0.05	0.18	0.16
	800	1.76	25.16	0.06	0.22	0.14
	1000	2.21	34.16	0.08	0.30	0.16
	1200	2.65	46.16	0.10	0.41	0.18
	1400	3.09	54.66	0.12	0.49	0.19
	1600	3.53	65.16	0.14	0.58	0.20
	1800	3.97	70.66	0.16	0.63	0.19
	2000	4.41	77.66	0.17	0.69	0.19
					Avg	0.17
					Sd(n-1)	0.017
					n	9

Table 10 (cont'd)

B-B4	contact ang	44.25	degree			
	$r_t=$	0.514	in	$T=1.0755$	$E= 0.9790$	
	$p=$	0.167	in	(1 in/6 thrd)		
	$d=$	4.048	in			
Run 1	CW	28 mm	Black			
	F_v, g	F_v, lb	F, g	F, lb	$T, in-lb$	μ_{cw}
	400	0.88	11.66	0.03	0.10	0.20
	600	1.32	18.66	0.04	0.17	0.22
	800	1.76	22.16	0.05	0.20	0.20
	1000	2.21	20.66	0.05	0.18	0.15
	1200	2.65	28.16	0.06	0.25	0.17
	1400	3.09	27.66	0.06	0.25	0.15
	1600	3.53	33.66	0.07	0.30	0.16
	1800	3.97	39.16	0.09	0.35	0.16
	2000	4.41	48.16	0.11	0.43	0.17
					Avg	0.18
					Sd(n-1)	0.024
					n	9

B-B4	contact ang	44.25	degree			
	$r_t=$	0.514	in	$T=1.0755$	$E= 0.9790$	
	$p=$	0.167	in	(1 in/6 thrd)		
	$d=$	4.048	in			
Run 1	CCW	28 mm	Black			
	F_v, g	F_v, lb	F, g	F, lb	$T, in-lb$	μ_{ccw}
	400	0.88	14.66	0.03	0.13	0.17
	600	1.32	21.16	0.05	0.19	0.16
	800	1.76	27.66	0.06	0.25	0.16
	1000	2.21	36.16	0.08	0.32	0.16
	1200	2.65	44.16	0.10	0.39	0.17
	1400	3.09	49.66	0.11	0.44	0.16
	1600	3.53	62.66	0.14	0.56	0.18
	1800	3.97	68.66	0.15	0.61	0.18
	2000	4.41	73.16	0.16	0.65	0.17
					Avg	0.17
					Sd(n-1)	0.008
					n	9

Table 10 (cont'd)

B-B4	contact ang	44.25	degree			
	r_t =	0.514	in	T=1.0755	E= 0.9790	
	p=	0.167	in	(1 in/6 thrd)		
	d=	4.048	in			
Run 2	CW	28 mm	Black			
	F_v , g	F_v , lb	F, g	F, lb	T, in-lb	μ_{cw}
	400	0.88	10.16	0.02	0.09	0.18
	600	1.32	13.16	0.03	0.12	0.16
	800	1.76	17.16	0.04	0.15	0.16
	1000	2.21	21.16	0.05	0.19	0.16
	1200	2.65	25.16	0.06	0.22	0.16
	1400	3.09	29.16	0.06	0.26	0.16
	1600	3.53	33.16	0.07	0.30	0.16
	1800	3.97	39.16	0.09	0.35	0.16
	2000	4.41	47.16	0.10	0.42	0.17
					Avg	0.16
					Sd(n-1)	0.009
					n	9

B-B4	contact ang	44.25	degree			
	r_t =	0.514	in	T=1.0755	E= 0.9790	
	p=	0.167	in	(1 in/6 thrd)		
	d=	4.048	in			
Run 2	CCW	28 mm	Black			
	F_v , g	F_v , lb	F, g	F, lb	T, in-lb	μ_{ccw}
	400	0.88	12.66	0.03	0.11	0.14
	600	1.32	24.16	0.05	0.22	0.19
	800	1.76	27.66	0.06	0.25	0.16
	1000	2.21	34.66	0.08	0.31	0.16
	1200	2.65	45.66	0.10	0.41	0.17
	1400	3.09	56.16	0.12	0.50	0.19
	1600	3.53	59.16	0.13	0.53	0.17
	1800	3.97	66.16	0.15	0.59	0.17
	2000	4.41	81.16	0.18	0.72	0.19
					Avg	0.17
					Sd(n-1)	0.017
					n	9

Table 10 (cont'd)

B-B4	contact ang	44.25	degree			
	r_t =	0.514	in	T=1.0755	E= 0.9790	
	p=	0.167	in	(1 in/6 thrd)		
	d=	4.048	in			
Run 3	CW	28 mm	Black			
	F_v , g	F_v , lb	F, g	F, lb	T, in-lb	μ_{cw}
	400	0.88	13.16	0.03	0.12	0.23
	600	1.32	16.16	0.04	0.14	0.19
	800	1.76	19.16	0.04	0.17	0.17
	1000	2.21	24.16	0.05	0.22	0.18
	1200	2.65	30.66	0.07	0.27	0.18
	1400	3.09	31.16	0.07	0.28	0.16
	1600	3.53	32.66	0.07	0.29	0.15
	1800	3.97	39.16	0.09	0.35	0.16
	2000	4.41	47.16	0.10	0.42	0.17
					Avg	0.18
					Sd(n-1)	0.021
					n	9

B-B4	contact ang	44.25	degree			
	r_t =	0.514	in	T=1.0755	E= 0.9790	
	p=	0.167	in	(1 in/6 thrd)		
	d=	4.048	in			
Run 3	CCW	28 mm	Black			
	F_v , g	F_v , lb	F, g	F, lb	T, in-lb	μ_{ccw}
	400	0.88	15.66	0.03	0.14	0.18
	600	1.32	24.16	0.05	0.22	0.19
	800	1.76	31.16	0.07	0.28	0.18
	1000	2.21	36.16	0.08	0.32	0.16
	1200	2.65	43.16	0.10	0.39	0.16
	1400	3.09	60.16	0.13	0.54	0.20
	1600	3.53	59.16	0.13	0.53	0.17
	1800	3.97	65.66	0.14	0.59	0.17
	2000	4.41	78.16	0.17	0.70	0.18
					Avg	0.18
					Sd(n-1)	0.013
					n	9

Table 10 (cont'd)

B-B4	contact ang	44.25	degree			
	r_t =	0.514	in	T=1.0755	E= 0.9790	
	p=	0.167	in	(1 in/6 thrd)		
	d=	4.048	in			
Run 4	CW	28 mm	Black			
	F_v , g	F_v , lb	F, g	F, lb	T, in-lb	μ_{cw}
	400	0.88	7.66	0.02	0.07	0.15
	600	1.32	11.66	0.03	0.10	0.15
	800	1.76	19.66	0.04	0.18	0.18
	1000	2.21	23.66	0.05	0.21	0.17
	1200	2.65	27.66	0.06	0.25	0.17
	1400	3.09	30.66	0.07	0.27	0.16
	1600	3.53	36.66	0.08	0.33	0.17
	1800	3.97	38.16	0.08	0.34	0.16
	2000	4.41	47.66	0.11	0.43	0.17
					Avg	0.16
					Sd(n-1)	0.011
					n	9

B-B4	contact ang	44.25	degree			
	r_t =	0.514	in	T=1.0755	E= 0.9790	
	p=	0.167	in	(1 in/6 thrd)		
	d=	4.048	in			
Run 4	CCW	28 mm	Black			
	F_v , g	F_v , lb	F, g	F, lb	T, in-lb	μ_{ccw}
	400	0.88	17.66	0.04	0.16	0.21
	600	1.32	21.16	0.05	0.19	0.16
	800	1.76	26.66	0.06	0.24	0.15
	1000	2.21	35.66	0.08	0.32	0.16
	1200	2.65	41.66	0.09	0.37	0.16
	1400	3.09	56.66	0.12	0.51	0.19
	1600	3.53	60.66	0.13	0.54	0.17
	1800	3.97	67.66	0.15	0.60	0.17
	2000	4.41	78.66	0.17	0.70	0.18
					Avg	0.17
					Sd(n-1)	0.018
					n	9

Table 10 (cont'd)

B-B4	contact ang	44.25	degree			
	r_t =	0.514	in	T=1.0755	E= 0.9790	
	p=	0.167	in	(1 in/6 thrd)		
	d=	4.048	in			
Run 5	CW	28 mm	Black			
	F_v , g	F_v , lb	F, g	F, lb	T, in-lb	μ_{cw}
	400	0.88	11.16	0.02	0.10	0.20
	600	1.32	12.16	0.03	0.11	0.15
	800	1.76	18.66	0.04	0.17	0.17
	1000	2.21	25.16	0.06	0.22	0.18
	1200	2.65	23.66	0.05	0.21	0.15
	1400	3.09	31.66	0.07	0.28	0.17
	1600	3.53	33.66	0.07	0.30	0.16
	1800	3.97	41.66	0.09	0.37	0.17
	2000	4.41	46.16	0.10	0.41	0.17
					Avg	0.17
					Sd(n-1)	0.015
					n	9

B-B5	contact ang	44.25	degree			
	r_t =	0.514	in	T=1.0755	E= 0.9790	
	p=	0.167	in	(1 in/6 thrd)		
	d=	4.048	in			
Run 5	CCW	28 mm	Black			
	F_v , g	F_v , lb	F, g	F, lb	T, in-lb	μ_{ccw}
	400	0.88	17.66	0.04	0.16	0.21
	600	1.32	19.16	0.04	0.17	0.14
	800	1.76	30.16	0.07	0.27	0.17
	1000	2.21	33.16	0.07	0.30	0.15
	1200	2.65	45.16	0.10	0.40	0.17
	1400	3.09	51.66	0.11	0.46	0.17
	1600	3.53	60.66	0.13	0.54	0.17
	1800	3.97	66.66	0.15	0.59	0.17
	2000	4.41	78.66	0.17	0.70	0.18
					Avg	0.17
					Sd(n-1)	0.019
					n	9

Table 10 (cont'd)

B-B6	contact ang	20	degree			
	r_t =	0.514	in	T=1.0755	E= 0.9790	
	p=	0.167	in	(1 in/6 thrd)		
	d=	4.048	in			
Run 1	CW	28 mm	Black			
	F_v , g	F_v , lb	F, g	F, lb	T, in-lb	μ_{cw}
	400	0.88	6.66	0.01	0.06	0.17
	600	1.32	11.66	0.03	0.10	0.19
	800	1.76	15.16	0.03	0.14	0.19
	1000	2.21	22.66	0.05	0.20	0.22
	1200	2.65	20.16	0.04	0.18	0.17
	1400	3.09	27.16	0.06	0.24	0.19
	1600	3.53	25.16	0.06	0.22	0.17
	1800	3.97	30.16	0.07	0.27	0.17
	2000	4.41	34.66	0.08	0.31	0.18
					Avg	0.18
					Sd(n-1)	0.016
					n	9

B-B6	contact ang	20	degree			
	r_t =	0.514	in	T=1.0755	E= 0.9790	
	p=	0.167	in	(1 in/6 thrd)		
	d=	4.048	in			
Run 1	CCW	28 mm	Black			
	F_v , g	F_v , lb	F, g	F, lb	T, in-lb	μ_{ccw}
	400	0.88	15.16	0.03	0.14	0.23
	600	1.32	20.66	0.05	0.18	0.20
	800	1.76	25.16	0.06	0.22	0.18
	1000	2.21	31.66	0.07	0.28	0.18
	1200	2.65	39.66	0.09	0.35	0.19
	1400	3.09	44.16	0.10	0.39	0.18
	1600	3.53	48.16	0.11	0.43	0.17
	1800	3.97	50.16	0.11	0.45	0.16
	2000	4.41	55.66	0.12	0.50	0.16
					Avg	0.18
					Sd(n-1)	0.023
					n	9

Table 10 (cont'd)

B-B6	contact ang	20	degree			
	r _t =	0.514	in	T=1.0755	E= 0.9790	
	p=	0.167	in	(1 in/6 thrd)		
	d=	4.048	in			
Run 2	CW	28 mm	Black			
	F _v , g	F _v , lb	F, g	F, lb	T, in-lb	μ _{cw}
	400	0.88	5.16	0.01	0.05	0.14
	600	1.32	10.66	0.02	0.10	0.18
	800	1.76	14.16	0.03	0.13	0.18
	1000	2.21	18.16	0.04	0.16	0.18
	1200	2.65	21.16	0.05	0.19	0.18
	1400	3.09	22.66	0.05	0.20	0.17
	1600	3.53	30.16	0.07	0.27	0.19
	1800	3.97	32.16	0.07	0.29	0.18
	2000	4.41	35.16	0.08	0.31	0.18
					Avg	0.18
					Sd(n-1)	0.013
					n	9

B-B6	contact ang	20	degree			
	r _t =	0.514	in	T=1.0755	E= 0.9790	
	p=	0.167	in	(1 in/6 thrd)		
	d=	4.048	in			
Run 2	CCW	28 mm	Black			
	F _v , g	F _v , lb	F, g	F, lb	T, in-lb	μ _{ccw}
	400	0.88	16.16	0.04	0.14	0.25
	600	1.32	22.16	0.05	0.20	0.22
	800	1.76	30.16	0.07	0.27	0.23
	1000	2.21	35.16	0.08	0.31	0.21
	1200	2.65	41.66	0.09	0.37	0.21
	1400	3.09	49.16	0.11	0.44	0.21
	1600	3.53	53.16	0.12	0.47	0.19
	1800	3.97	41.16	0.09	0.37	0.12
	2000	4.41	68.16	0.15	0.61	0.20
					Avg	0.20
					Sd(n-1)	0.035
					n	9

Table 10 (cont'd)

B-B6	contact ang	20	degree			
	r_t =	0.514	in	T=1.0755	E= 0.9790	
	p=	0.167	in	(1 in/6 thrd)		
	d=	4.048	in			
Run 3	CW	28 mm	Black			
	F_v , g	F_v , lb	F, g	F, lb	T, in-lb	μ_{cw}
	400	0.88	7.16	0.02	0.06	0.18
	600	1.32	10.16	0.02	0.09	0.18
	800	1.76	14.66	0.03	0.13	0.19
	1000	2.21	20.66	0.05	0.18	0.20
	1200	2.65	25.66	0.06	0.23	0.21
	1400	3.09	20.66	0.05	0.18	0.16
	1600	3.53	26.16	0.06	0.23	0.17
	1800	3.97	28.16	0.06	0.25	0.17
	2000	4.41	31.66	0.07	0.28	0.17
					Avg	0.18
					Sd(n-1)	0.017
					n	9

B-B6	contact ang	20	degree			
	r_t =	0.514	in	T=1.0755	E= 0.9790	
	p=	0.167	in	(1 in/6 thrd)		
	d=	4.048	in			
Run 3	CCW	28 mm	Black			
	F_v , g	F_v , lb	F, g	F, lb	T, in-lb	μ_{ccw}
	400	0.88	15.16	0.03	0.14	0.23
	600	1.32	21.16	0.05	0.19	0.21
	800	1.76	26.16	0.06	0.23	0.19
	1000	2.21	32.16	0.07	0.29	0.19
	1200	2.65	38.16	0.08	0.34	0.18
	1400	3.09	43.16	0.10	0.39	0.18
	1600	3.53	49.66	0.11	0.44	0.18
	1800	3.97	58.16	0.13	0.52	0.19
	2000	4.41	64.66	0.14	0.58	0.19
					Avg	0.19
					Sd(n-1)	0.016
					n	9

Table 10 (cont'd)

B-B6	contact ang	20	degree			
	r_t =	0.514	in	T=1.0755	E= 0.9790	
	p=	0.167	in	(1 in/6 thrd)		
	d=	4.048	in			
Run 4	CW	28 mm	Black			
	F_v , g	F_v , lb	F, g	F, lb	T, in-lb	μ_{cw}
	400	0.88	9.66	0.02	0.09	0.23
	600	1.32	12.66	0.03	0.11	0.21
	800	1.76	16.66	0.04	0.15	0.20
	1000	2.21	16.66	0.04	0.15	0.17
	1200	2.65	23.66	0.05	0.21	0.20
	1400	3.09	22.16	0.05	0.20	0.17
	1600	3.53	26.16	0.06	0.23	0.17
	1800	3.97	27.66	0.06	0.25	0.16
	2000	4.41	31.66	0.07	0.28	0.17
					Avg	0.19
					Sd(n-1)	0.023
					n	9

B-B6	contact ang	20	degree			
	r_t =	0.514	in	T=1.0755	E= 0.9790	
	p=	0.167	in	(1 in/6 thrd)		
	d=	4.048	in			
Run 4	CCW	28 mm	Black			
	F_v , g	F_v , lb	F, g	F, lb	T, in-lb	μ_{ccw}
	400	0.88	14.66	0.03	0.13	0.22
	600	1.32	20.16	0.04	0.18	0.20
	800	1.76	25.16	0.06	0.22	0.18
	1000	2.21	31.16	0.07	0.28	0.18
	1200	2.65	36.16	0.08	0.32	0.17
	1400	3.09	41.66	0.09	0.37	0.17
	1600	3.53	48.16	0.11	0.43	0.17
	1800	3.97	53.66	0.12	0.48	0.17
	2000	4.41	61.16	0.13	0.55	0.18
					Avg	0.18
					Sd(n-1)	0.016
					n	9

Table 10 (cont'd)

B-B6	contact ang	20	degree			
	r_t =	0.514	in	T=1.0755	E= 0.9790	
	p=	0.167	in	(1 in/6 thrd)		
	d=	4.048	in			
Run 5	CW	28 mm	Black			
	F_v , g	F_v , lb	F, g	F, lb	T, in-lb	μ_{cw}
	400	0.88	5.16	0.01	0.05	0.14
	600	1.32	9.16	0.02	0.08	0.16
	800	1.76	10.16	0.02	0.09	0.14
	1000	2.21	19.16	0.04	0.17	0.19
	1200	2.65	20.66	0.05	0.18	0.18
	1400	3.09	23.66	0.05	0.21	0.17
	1600	3.53	26.66	0.06	0.24	0.17
	1800	3.97	31.16	0.07	0.28	0.18
	2000	4.41	37.66	0.08	0.34	0.19
					Avg	0.17
					Sd(n-1)	0.017
					n	9

B-B6	contact ang	20	degree			
	r_t =	0.514	in	T=1.0755	E= 0.9790	
	p=	0.167	in	(1 in/6 thrd)		
	d=	4.048	in			
Run 5	CCW	28 mm	Black			
	F_v , g	F_v , lb	F, g	F, lb	T, in-lb	μ_{ccw}
	400	0.88	14.16	0.03	0.13	0.21
	600	1.32	20.66	0.05	0.18	0.20
	800	1.76	26.16	0.06	0.23	0.19
	1000	2.21	32.16	0.07	0.29	0.19
	1200	2.65	38.16	0.08	0.34	0.18
	1400	3.09	43.66	0.10	0.39	0.18
	1600	3.53	49.16	0.11	0.44	0.18
	1800	3.97	56.16	0.12	0.50	0.18
	2000	4.41	62.16	0.14	0.55	0.18
					Avg	0.19
					Sd(n-1)	0.012
					n	9

Table 10 (cont'd)

C-C1	contact ang	41.5	degree			
	r_t =	0.7059	in	T=1.4630	E= 1.3605	
	p=	0.167	in	(1 in/6 thrd)		
	d=	4.048	in			
Run 1	CW	38 mm	White			
	F_v , g	F_v , lb	F, g	F, lb	T, in-lb	μ_{cw}
	400	0.88	8.16	0.02	0.07	0.12
	600	1.32	12.16	0.03	0.11	0.12
	800	1.76	14.66	0.03	0.13	0.11
	1000	2.21	17.66	0.04	0.16	0.10
	1200	2.65	20.16	0.04	0.18	0.10
	1400	3.09	23.16	0.05	0.21	0.10
	1600	3.53	26.16	0.06	0.23	0.10
	1800	3.97	29.66	0.07	0.26	0.10
	2000	4.41	32.66	0.07	0.29	0.10
					Avg	0.10
					Sd(n-1)	0.007
					n	9

C-C1	contact ang	41.5	degree			
	r_t =	0.7059	in	T=1.4630	E= 1.3605	
	p=	0.167	in	(1 in/6 thrd)		
	d=	4.048	in			
Run 1	CCW	38 mm	White			
	F_v , g	F_v , lb	F, g	F, lb	T, in-lb	μ_{ccw}
	400	0.88	14.16	0.03	0.13	0.12
	600	1.32	19.16	0.04	0.17	0.11
	800	1.76	26.16	0.06	0.23	0.11
	1000	2.21	33.16	0.07	0.30	0.11
	1200	2.65	35.66	0.08	0.32	0.10
	1400	3.09	44.16	0.10	0.39	0.11
	1600	3.53	53.66	0.12	0.48	0.12
	1800	3.97	60.66	0.13	0.54	0.12
	2000	4.41	67.16	0.15	0.60	0.12
					Avg	0.11
					Sd(n-1)	0.007
					n	9

Table 10 (cont'd)

C-C1	contact ang	41.5	degree			
	r_t =	0.7059	in	T=1.4630	E= 1.3605	
	p=	0.167	in	(1 in/6 thrd)		
	d=	4.048	in			
Run 2	CW	38 mm	White			
	F_v , g	F_v , lb	F, g	F, lb	T, in-lb	μ_{cw}
	400	0.88	7.66	0.02	0.07	0.11
	600	1.32	13.66	0.03	0.12	0.13
	800	1.76	16.16	0.04	0.14	0.12
	1000	2.21	16.16	0.04	0.14	0.10
	1200	2.65	23.66	0.05	0.21	0.11
	1400	3.09	27.66	0.06	0.25	0.11
	1600	3.53	29.66	0.07	0.26	0.11
	1800	3.97	32.66	0.07	0.29	0.11
	2000	4.41	32.66	0.07	0.29	0.10
					Avg	0.11
					Sd(n-1)	0.009
					n	9

C-C1	contact ang	41.5	degree			
	r_t =	0.7059	in	T=1.4630	E= 1.3605	
	p=	0.167	in	(1 in/6 thrd)		
	d=	4.048	in			
Run 2	CCW	38 mm	White			
	F_v , g	F_v , lb	F, g	F, lb	T, in-lb	μ_{ccw}
	400	0.88	14.66	0.03	0.13	0.13
	600	1.32	24.16	0.05	0.22	0.14
	800	1.76	23.16	0.05	0.21	0.10
	1000	2.21	38.66	0.09	0.35	0.14
	1200	2.65	37.66	0.08	0.34	0.11
	1400	3.09	42.66	0.09	0.38	0.10
	1600	3.53	51.66	0.11	0.46	0.11
	1800	3.97	65.66	0.14	0.59	0.13
	2000	4.41	69.66	0.15	0.62	0.12
					Avg	0.12
					Sd(n-1)	0.016
					n	9

Table 10 (cont'd)

C-C1	contact ang	41.5	degree			
	r_t =	0.7059	in	T=1.4630	E= 1.3605	
	p=	0.167	in	(1 in/6 thrd)		
	d=	4.048	in			
Run 3	CW	38 mm	White			
	F_v , g	F_v , lb	F, g	F, lb	T, in-lb	μ_{cw}
	400	0.88	5.66	0.01	0.05	0.09
	600	1.32	14.16	0.03	0.13	0.13
	800	1.76	14.66	0.03	0.13	0.11
	1000	2.21	19.66	0.04	0.18	0.11
	1200	2.65	19.66	0.04	0.18	0.10
	1400	3.09	31.16	0.07	0.28	0.12
	1600	3.53	25.16	0.06	0.22	0.10
	1800	3.97	31.66	0.07	0.28	0.10
	2000	4.41	33.16	0.07	0.30	0.10
					Avg	0.11
					Sd(n-1)	0.013
					n	9

C-C1	contact ang	41.5	degree			
	r_t =	0.7059	in	T=1.4630	E= 1.3605	
	p=	0.167	in	(1 in/6 thrd)		
	d=	4.048	in			
Run 3	CCW	38 mm	White			
	F_v , g	F_v , lb	F, g	F, lb	T, in-lb	μ_{ccw}
	400	0.88	18.16	0.04	0.16	0.17
	600	1.32	22.16	0.05	0.20	0.13
	800	1.76	29.66	0.07	0.26	0.13
	1000	2.21	31.66	0.07	0.28	0.11
	1200	2.65	34.66	0.08	0.31	0.10
	1400	3.09	43.66	0.10	0.39	0.11
	1600	3.53	56.66	0.12	0.51	0.12
	1800	3.97	63.66	0.14	0.57	0.12
	2000	4.41	65.66	0.14	0.59	0.11
					Avg	0.12
					Sd(n-1)	0.020
					n	9

Table 10 (cont'd)

C-C1	contact ang	41.5	degree			
	r_t =	0.7059	in	T=1.4630	E= 1.3605	
	p=	0.167	in	(1 in/6 thrd)		
	d=	4.048	in			
Run 4	CW	38 mm	White			
	F_v , g	F_v , lb	F, g	F, lb	T, in-lb	μ_{cw}
	400	0.88	8.16	0.02	0.07	0.12
	600	1.32	11.66	0.03	0.10	0.11
	800	1.76	16.66	0.04	0.15	0.12
	1000	2.21	20.66	0.05	0.18	0.12
	1200	2.65	15.66	0.03	0.14	0.08
	1400	3.09	25.66	0.06	0.23	0.11
	1600	3.53	28.66	0.06	0.26	0.11
	1800	3.97	32.66	0.07	0.29	0.11
	2000	4.41	34.16	0.08	0.30	0.10
					Avg	0.11
					Sd(n-1)	0.010
					n	9

C-C1	contact ang	41.5	degree			
	r_t =	0.7059	in	T=1.4630	E= 1.3605	
	p=	0.167	in	(1 in/6 thrd)		
	d=	4.048	in			
Run 4	CCW	38 mm	White			
	F_v , g	F_v , lb	F, g	F, lb	T, in-lb	μ_{ccw}
	400	0.88	17.16	0.04	0.15	0.15
	600	1.32	19.66	0.04	0.18	0.11
	800	1.76	23.66	0.05	0.21	0.10
	1000	2.21	32.66	0.07	0.29	0.11
	1200	2.65	39.66	0.09	0.35	0.11
	1400	3.09	45.66	0.10	0.41	0.11
	1600	3.53	50.16	0.11	0.45	0.11
	1800	3.97	58.16	0.13	0.52	0.11
	2000	4.41	66.66	0.15	0.59	0.11
					Avg	0.11
					Sd(n-1)	0.016
					n	9

Table 10 (cont'd)

C-C1	contact ang	41.5	degree			
	r_t =	0.7059	in	T=1.4630	E= 1.3605	
	p=	0.167	in	(1 in/6 thrd)		
	d=	4.048	in			
Run 5	CW	38 mm	White			
	F_v , g	F_v , lb	F, g	F, lb	T, in-lb	μ_{cw}
	400	0.88	10.16	0.02	0.09	0.14
	600	1.32	8.66	0.02	0.08	0.09
	800	1.76	16.66	0.04	0.15	0.12
	1000	2.21	17.66	0.04	0.16	0.10
	1200	2.65	20.66	0.05	0.18	0.10
	1400	3.09	24.16	0.05	0.22	0.10
	1600	3.53	26.66	0.06	0.24	0.10
	1800	3.97	32.16	0.07	0.29	0.11
	2000	4.41	36.66	0.08	0.33	0.11
					Avg	0.11
					Sd(n-1)	0.013
					n	9

C-C1	contact ang	41.5	degree			
	r_t =	0.7059	in	T=1.4630	E= 1.3605	
	p=	0.167	in	(1 in/6 thrd)		
	d=	4.048	in			
Run 5	CCW	38 mm	White			
	F_v , g	F_v , lb	F, g	F, lb	T, in-lb	μ_{ccw}
	400	0.88	16.16	0.04	0.14	0.14
	600	1.32	21.66	0.05	0.19	0.13
	800	1.76	21.66	0.05	0.19	0.09
	1000	2.21	30.66	0.07	0.27	0.10
	1200	2.65	37.66	0.08	0.34	0.11
	1400	3.09	43.66	0.10	0.39	0.11
	1600	3.53	56.66	0.12	0.51	0.12
	1800	3.97	62.16	0.14	0.55	0.12
	2000	4.41	71.66	0.16	0.64	0.12
					Avg	0.12
					Sd(n-1)	0.017
					n	9

Table 10 (cont'd)

C-C2	contact ang	39.75	degree			
	r _t =	0.7059	in	T=1.4630	E= 1.3605	
	p=	0.167	in	(1 in/6 thrd)		
	d=	4.048	in			
Run 1	CW	38 mm	White			
	F _v , g	F _v , lb	F, g	F, lb	T, in-lb	μ _{cw}
	400	0.88	8.66	0.02	0.08	0.12
	600	1.32	10.66	0.02	0.10	0.11
	800	1.76	14.16	0.03	0.13	0.11
	1000	2.21	17.16	0.04	0.15	0.10
	1200	2.65	20.16	0.04	0.18	0.10
	1400	3.09	23.16	0.05	0.21	0.10
	1600	3.53	27.16	0.06	0.24	0.10
	1800	3.97	30.16	0.07	0.27	0.10
	2000	4.41	32.66	0.07	0.29	0.10
					Avg	0.11
					Sd(n-1)	0.007
					n	9

C-C2	contact ang	39.75	degree			
	r _t =	0.7059	in	T=1.4630	E= 1.3605	
	p=	0.167	in	(1 in/6 thrd)		
	d=	4.048	in			
Run 1	CCW	38 mm	White			
	F _v , g	F _v , lb	F, g	F, lb	T, in-lb	μ _{ccw}
	400	0.88	13.16	0.03	0.12	0.12
	600	1.32	18.16	0.04	0.16	0.10
	800	1.76	26.66	0.06	0.24	0.12
	1000	2.21	33.66	0.07	0.30	0.12
	1200	2.65	39.16	0.09	0.35	0.11
	1400	3.09	47.16	0.10	0.42	0.12
	1600	3.53	48.16	0.11	0.43	0.10
	1800	3.97	55.16	0.12	0.49	0.11
	2000	4.41	72.16	0.16	0.64	0.13
					Avg	0.11
					Sd(n-1)	0.009
					n	9

Table 10 (cont'd)

C-C2	contact ang	39.75	degree			
	r_t =	0.7059	in	T=1.4630	E= 1.3605	
	p=	0.167	in	(1 in/6 thrd)		
	d=	4.048	in			
Run 2	CW	38 mm	White			
	F_v , g	F_v , lb	F, g	F, lb	T, in-lb	μ_{cw}
	400	0.88	9.66	0.02	0.09	0.14
	600	1.32	10.16	0.02	0.09	0.10
	800	1.76	15.66	0.03	0.14	0.12
	1000	2.21	20.16	0.04	0.18	0.12
	1200	2.65	17.66	0.04	0.16	0.09
	1400	3.09	20.66	0.05	0.18	0.09
	1600	3.53	25.66	0.06	0.23	0.10
	1800	3.97	30.66	0.07	0.27	0.10
	2000	4.41	27.16	0.06	0.24	0.09
					Avg	0.11
					Sd(n-1)	0.015
					n	9

C-C2	contact ang	39.75	degree			
	r_t =	0.7059	in	T=1.4630	E= 1.3605	
	p=	0.167	in	(1 in/6 thrd)		
	d=	4.048	in			
Run 2	CCW	38 mm	White			
	F_v , g	F_v , lb	F, g	F, lb	T, in-lb	μ_{ccw}
	400	0.88	13.66	0.03	0.12	0.12
	600	1.32	20.66	0.05	0.18	0.12
	800	1.76	31.66	0.07	0.28	0.14
	1000	2.21	31.66	0.07	0.28	0.11
	1200	2.65	41.16	0.09	0.37	0.12
	1400	3.09	48.66	0.11	0.43	0.12
	1600	3.53	53.16	0.12	0.47	0.12
	1800	3.97	55.66	0.12	0.50	0.11
	2000	4.41	74.66	0.16	0.67	0.13
					Avg	0.12
					Sd(n-1)	0.012
					n	9

Table 10 (cont'd)

C-C2	contact ang	39.75	degree			
	r_t =	0.7059	in	T=1.4630	E= 1.3605	
	p=	0.167	in	(1 in/6 thrd)		
	d=	4.048	in			
Run 3	CW	38 mm	White			
	F_v , g	F_v , lb	F, g	F, lb	T, in-lb	μ_{cw}
	400	0.88	10.16	0.02	0.09	0.14
	600	1.32	11.66	0.03	0.10	0.12
	800	1.76	15.66	0.03	0.14	0.12
	1000	2.21	18.16	0.04	0.16	0.11
	1200	2.65	18.16	0.04	0.16	0.10
	1400	3.09	19.16	0.04	0.17	0.09
	1600	3.53	29.66	0.07	0.26	0.11
	1800	3.97	30.66	0.07	0.27	0.10
	2000	4.41	33.66	0.07	0.30	0.10
					Avg	0.11
					Sd(n-1)	0.015
					n	9

C-C2	contact ang	39.75	degree			
	r_t =	0.7059	in	T=1.4630	E= 1.3605	
	p=	0.167	in	(1 in/6 thrd)		
	d=	4.048	in			
Run 3	CCW	38 mm	White			
	F_v , g	F_v , lb	F, g	F, lb	T, in-lb	μ_{ccw}
	400	0.88	15.16	0.03	0.14	0.14
	600	1.32	16.16	0.04	0.14	0.09
	800	1.76	26.16	0.06	0.23	0.11
	1000	2.21	32.16	0.07	0.29	0.11
	1200	2.65	36.16	0.08	0.32	0.10
	1400	3.09	51.66	0.11	0.46	0.13
	1600	3.53	50.66	0.11	0.45	0.11
	1800	3.97	58.66	0.13	0.52	0.11
	2000	4.41	70.66	0.16	0.63	0.13
					Avg	0.12
					Sd(n-1)	0.015
					n	9

Table 10 (cont'd)

C-C2	contact ang	39.75	degree			
	r_t =	0.7059	in	T=1.4630	E= 1.3605	
	p=	0.167	in	(1 in/6 thrd)		
	d=	4.048	in			
Run 4	CW	38 mm	White			
	F_v , g	F_v , lb	F, g	F, lb	T, in-lb	μ_{cw}
	400	0.88	8.66	0.02	0.08	0.12
	600	1.32	10.66	0.02	0.10	0.11
	800	1.76	18.66	0.04	0.17	0.13
	1000	2.21	20.66	0.05	0.18	0.12
	1200	2.65	20.16	0.04	0.18	0.10
	1400	3.09	26.66	0.06	0.24	0.11
	1600	3.53	28.16	0.06	0.25	0.11
	1800	3.97	28.66	0.06	0.26	0.10
	2000	4.41	32.66	0.07	0.29	0.10
					Avg	0.11
					Sd(n-1)	0.011
					n	9

C-C2	contact ang	39.75	degree			
	r_t =	0.7059	in	T=1.4630	E= 1.3605	
	p=	0.167	in	(1 in/6 thrd)		
	d=	4.048	in			
Run 4	CCW	38 mm	White			
	F_v , g	F_v , lb	F, g	F, lb	T, in-lb	μ_{ccw}
	400	0.88	14.66	0.03	0.13	0.13
	600	1.32	20.16	0.04	0.18	0.12
	800	1.76	25.66	0.06	0.23	0.11
	1000	2.21	34.66	0.08	0.31	0.12
	1200	2.65	44.16	0.10	0.39	0.13
	1400	3.09	43.16	0.10	0.39	0.11
	1600	3.53	50.16	0.11	0.45	0.11
	1800	3.97	50.66	0.11	0.45	0.09
	2000	4.41	73.66	0.16	0.66	0.13
					Avg	0.12
					Sd(n-1)	0.013
					n	9

Table 10 (cont'd)

C-C2	contact ang	39.75	degree			
	r_t =	0.7059	in	T=1.4630	E= 1.3605	
	p=	0.167	in	(1 in/6 thrd)		
	d=	4.048	in			
Run 5	CW	38 mm	White			
	F_v , g	F_v , lb	F, g	F, lb	T, in-lb	μ_{cw}
	400	0.88	10.16	0.02	0.09	0.14
	600	1.32	10.66	0.02	0.10	0.11
	800	1.76	18.66	0.04	0.17	0.13
	1000	2.21	18.66	0.04	0.17	0.11
	1200	2.65	22.66	0.05	0.20	0.11
	1400	3.09	29.66	0.07	0.26	0.12
	1600	3.53	28.16	0.06	0.25	0.11
	1800	3.97	33.66	0.07	0.30	0.11
	2000	4.41	37.16	0.08	0.33	0.11
					Avg	0.12
					Sd(n-1)	0.012
					n	9

C-C2	contact ang	39.75	degree			
	r_t =	0.7059	in	T=1.4630	E= 1.3605	
	p=	0.167	in	(1 in/6 thrd)		
	d=	4.048	in			
Run 5	CCW	38 mm	White			
	F_v , g	F_v , lb	F, g	F, lb	T, in-lb	μ_{ccw}
	400	0.88	13.16	0.03	0.12	0.12
	600	1.32	20.16	0.04	0.18	0.12
	800	1.76	30.66	0.07	0.27	0.14
	1000	2.21	39.66	0.09	0.35	0.14
	1200	2.65	46.66	0.10	0.42	0.14
	1400	3.09	45.66	0.10	0.41	0.11
	1600	3.53	53.16	0.12	0.47	0.12
	1800	3.97	54.16	0.12	0.48	0.10
	2000	4.41	72.66	0.16	0.65	0.13
					Avg	0.12
					Sd(n-1)	0.014
					n	9

Table 11 Raw Data of the Static Coefficient of Friction at the Liner Interface

B-B1	E, in	0.979				
	l, in	0.838				
	r _s , in	0.45425				
	d, in	4.048				
Run 1	CW	28 mm	White	PE foam	glued	
	F _v , g	F _v , lb	F, g	F, lb	T, in-lb	μ _{cw}
	150	0.33	11.66	0.026	0.10	0.69
	200	0.44	16.16	0.036	0.14	0.72
	300	0.66	23.16	0.051	0.21	0.69
	400	0.88	33.16	0.073	0.30	0.74
	600	1.32	46.16	0.102	0.41	0.69
	800	1.76	68.16	0.150	0.61	0.76
					Avg	0.71
					Sd(n-1)	0.03
					n	6

B-B1	E, in	0.979				
	l, in	0.838				
	r _s , in	0.45425				
	d, in	4.048				
Run 1	CCW	28 mm	White	PE foam	glued	
	F _v , g	F _v , lb	F, g	F, lb	T, in-lb	μ _{ccw}
	150	0.33	11.16	0.025	0.10	0.66
	200	0.44	15.16	0.033	0.14	0.68
	300	0.66	22.16	0.049	0.20	0.66
	400	0.88	31.16	0.069	0.28	0.69
	600	1.32	43.16	0.095	0.39	0.64
	800	1.76	63.16	0.139	0.56	0.70
					Avg	0.67
					Sd(n-1)	0.02
					n	6

Table 11 (cont'd)

B-B1	E, in	0.979				
	l, in	0.838				
	r _s , in	0.45425				
	d, in	4.048				
Run 2	CW	28 mm	White	PE foam	glued	
	F _v , g	F _v , lb	F, g	F, lb	T, in-lb	μ _{cw}
	150	0.33	11.66	0.026	0.10	0.69
	200	0.44	16.16	0.036	0.14	0.72
	300	0.66	23.16	0.051	0.21	0.69
	400	0.88	33.16	0.073	0.30	0.74
	600	1.32	46.16	0.102	0.41	0.69
	800	1.76	68.16	0.150	0.61	0.76
					Avg	0.71
					Sd(n-1)	0.03
					n	6

B-B1	E, in	0.979				
	l, in	0.838				
	r _s , in	0.45425				
	d, in	4.048				
Run 2	CCW	28 mm	White	PE foam	glued	
	F _v , g	F _v , lb	F, g	F, lb	T, in-lb	μ _{ccw}
	150	0.33	15.16	0.033	0.14	0.90
	200	0.44	20.16	0.044	0.18	0.90
	300	0.66	28.16	0.062	0.25	0.84
	400	0.88	40.16	0.089	0.36	0.89
	600	1.32	48.16	0.106	0.43	0.72
	800	1.76	74.16	0.164	0.66	0.83
					Avg	0.85
					Sd(n-1)	0.07
					n	6

Table 11 (cont'd)

B-B1	E, in	0.979				
	l, in	0.838				
	r _s , in	0.45425				
	d, in	4.048				
Run 3	CW	28 mm	White	PE foam	glued	
	F _v , g	F _v , lb	F, g	F, lb	T, in-lb	μ _{cw}
	150	0.33	14.16	0.031	0.13	0.84
	200	0.44	15.66	0.035	0.14	0.70
	300	0.66	25.16	0.055	0.22	0.75
	400	0.88	40.16	0.089	0.36	0.89
	600	1.32	44.16	0.097	0.39	0.66
	800	1.76	70.16	0.155	0.63	0.78
					Avg	0.77
					Sd(n-1)	0.09
					n	6

B-B1	E, in	0.979				
	l, in	0.838				
	r _s , in	0.45425				
	d, in	4.048				
Run 3	CCW	28 mm	White	PE foam	glued	
	F _v , g	F _v , lb	F, g	F, lb	T, in-lb	μ _{ccw}
	150	0.33	14.16	0.031	0.13	0.84
	200	0.44	17.66	0.039	0.16	0.79
	300	0.66	25.66	0.057	0.23	0.76
	400	0.88	34.16	0.075	0.30	0.76
	600	1.32	46.66	0.103	0.42	0.69
	800	1.76	73.66	0.162	0.66	0.82
					Avg	0.78
					Sd(n-1)	0.05
					n	6

Table 11 (cont'd)

B-B1	E, in	0.979				
	l, in	0.838				
	r _s , in	0.45425				
	d, in	4.048				
Run 4	CW	28 mm	White	PE foam	glued	
	F _v , g	F _v , lb	F, g	F, lb	T, in-lb	μ _{cw}
	150	0.33	12.66	0.028	0.11	0.75
	200	0.44	14.66	0.032	0.13	0.65
	300	0.66	25.66	0.057	0.23	0.76
	400	0.88	34.66	0.076	0.31	0.77
	600	1.32	47.16	0.104	0.42	0.70
	800	1.76	65.16	0.144	0.58	0.73
					Avg	0.73
					Sd(n-1)	0.04
					n	6

B-B1	E, in	0.979				
	l, in	0.838				
	r _s , in	0.45425				
	d, in	4.048				
Run 4	CCW	28 mm	White	PE foam	glued	
	F _v , g	F _v , lb	F, g	F, lb	T, in-lb	μ _{ccw}
	150	0.33	12.66	0.028	0.11	0.75
	200	0.44	19.16	0.042	0.17	0.85
	300	0.66	23.66	0.052	0.21	0.70
	400	0.88	38.16	0.084	0.34	0.85
	600	1.32	47.16	0.104	0.42	0.70
	800	1.76	74.66	0.165	0.67	0.83
					Avg	0.78
					Sd(n-1)	0.07
					n	6

Table 11 (cont'd)

B-B1	E, in	0.979				
	l, in	0.838				
	r _s , in	0.45425				
	d, in	4.048				
Run 5	CW	28 mm	White	PE foam	glued	
	F _v , g	F _v , lb	F, g	F, lb	T, in-lb	μ _{cw}
	150	0.33	11.66	0.026	0.10	0.69
	200	0.44	20.16	0.044	0.18	0.90
	300	0.66	23.66	0.052	0.21	0.70
	400	0.88	37.66	0.083	0.34	0.84
	600	1.32	48.66	0.107	0.43	0.72
	800	1.76	66.66	0.147	0.59	0.74
					Avg	0.77
					Sd(n-1)	0.08
					n	6

B-B1	E, in	0.979				
	l, in	0.838				
	r _s , in	0.45425				
	d, in	4.048				
Run 5	CCW	28 mm	White	PE foam	glued	
	F _v , g	F _v , lb	F, g	F, lb	T, in-lb	μ _{ccw}
	150	0.33	12.66	0.028	0.11	0.75
	200	0.44	17.16	0.038	0.15	0.76
	300	0.66	23.66	0.052	0.21	0.70
	400	0.88	28.66	0.063	0.26	0.64
	600	1.32	42.66	0.094	0.38	0.63
	800	1.76	72.66	0.160	0.65	0.81
					Avg	0.72
					Sd(n-1)	0.07
					n	6

Table 11 (cont'd)

B-B2	E, in	0.979				
	l, in	0.838				
	r _s , in	0.45425				
	d, in	4.048				
Run 1	CW	28 mm	White	PE foam	Non-glued	
	F _v , g	F _v , lb	F, g	F, lb	T, in-lb	μ _{cw}
	150	0.33	7.16	0.016	0.06	0.43
	200	0.44	10.16	0.022	0.09	0.45
	300	0.66	15.16	0.033	0.14	0.45
	400	0.88	22.16	0.049	0.20	0.49
	600	1.32	33.16	0.073	0.30	0.49
	800	1.76	45.66	0.101	0.41	0.51
					Avg	0.47
					Sd(n-1)	0.03
					n	6

B-B2	E, in	0.979				
	l, in	0.838				
	r _s , in	0.45425				
	d, in	4.048				
Run 1	CCW	28 mm	White	PE foam	Non-glued	
	F _v , g	F _v , lb	F, g	F, lb	T, in-lb	μ _{ccw}
	150	0.33	7.16	0.016	0.06	0.43
	200	0.44	10.16	0.022	0.09	0.45
	300	0.66	16.16	0.036	0.14	0.48
	400	0.88	23.16	0.051	0.21	0.52
	600	1.32	33.16	0.073	0.30	0.49
	800	1.76	46.66	0.103	0.42	0.52
					Avg	0.48
					Sd(n-1)	0.04
					n	6

Table 11 (cont'd)

B-B2	E, in	0.979				
	l, in	0.838				
	r _s , in	0.45425				
	d, in	4.048				
Run 2	CW	28 mm	White	PE foam	Non-glued	
	F _v , g	F _v , lb	F, g	F, lb	T, in-lb	μ _{cw}
	150	0.33	9.16	0.020	0.08	0.54
	200	0.44	12.16	0.027	0.11	0.54
	300	0.66	17.16	0.038	0.15	0.51
	400	0.88	23.16	0.051	0.21	0.52
	600	1.32	33.16	0.073	0.30	0.49
	800	1.76	46.16	0.102	0.41	0.51
					Avg	0.52
					Sd(n-1)	0.02
					n	6

B-B2	E, in	0.979				
	l, in	0.838				
	r _s , in	0.45425				
	d, in	4.048				
Run 2	CCW	28 mm	White	PE foam	Non-glued	
	F _v , g	F _v , lb	F, g	F, lb	T, in-lb	μ _{ccw}
	150	0.33	9.66	0.021	0.09	0.57
	200	0.44	13.16	0.029	0.12	0.59
	300	0.66	18.16	0.040	0.16	0.54
	400	0.88	24.16	0.053	0.22	0.54
	600	1.32	35.16	0.078	0.31	0.52
	800	1.76	47.16	0.104	0.42	0.53
					Avg	0.55
					Sd(n-1)	0.03
					n	6

Table 11 (cont'd)

B-B2	E, in	0.979				
	l, in	0.838				
	r _s , in	0.45425				
	d, in	4.048				
Run 3	CW	28 mm	White	PE foam	Non-glued	
	F _v , g	F _v , lb	F, g	F, lb	T, in-lb	μ _{cw}
	150	0.33	9.16	0.020	0.08	0.54
	200	0.44	10.16	0.022	0.09	0.45
	300	0.66	17.16	0.038	0.15	0.51
	400	0.88	23.16	0.051	0.21	0.52
	600	1.32	33.16	0.073	0.30	0.49
	800	1.76	46.16	0.102	0.41	0.51
					Avg	0.50
					Sd(n-1)	0.03
					n	6

B-B2	E, in	0.979				
	l, in	0.838				
	r _s , in	0.45425				
	d, in	4.048				
Run 3	CCW	28 mm	White	PE foam	Non-glued	
	F _v , g	F _v , lb	F, g	F, lb	T, in-lb	μ _{ccw}
	150	0.33	7.56	0.017	0.07	0.45
	200	0.44	10.66	0.024	0.10	0.47
	300	0.66	17.16	0.038	0.15	0.51
	400	0.88	22.66	0.050	0.20	0.50
	600	1.32	33.16	0.073	0.30	0.49
	800	1.76	44.66	0.098	0.40	0.50
					Avg	0.49
					Sd(n-1)	0.02
					n	6

Table 11 (cont'd)

B-B2	E, in	0.979				
	l, in	0.838				
	r _s , in	0.45425				
	d, in	4.048				
Run 4	CW	28 mm	White	PE foam	Non-glued	
	F _v , g	F _v , lb	F, g	F, lb	T, in-lb	μ _{CW}
	150	0.33	7.38	0.016	0.07	0.44
	200	0.44	11.66	0.026	0.10	0.52
	300	0.66	17.16	0.038	0.15	0.51
	400	0.88	23.66	0.052	0.21	0.53
	600	1.32	32.66	0.072	0.29	0.49
	800	1.76	47.16	0.104	0.42	0.53
					Avg	0.50
					Sd(n-1)	0.03
					n	6

B-B2	E, in	0.979				
	l, in	0.838				
	r _s , in	0.45425				
	d, in	4.048				
Run 4	CCW	28 mm	White	PE foam	Non-glued	
	F _v , g	F _v , lb	F, g	F, lb	T, in-lb	μ _{CCW}
	150	0.33	8.16	0.018	0.07	0.48
	200	0.44	10.16	0.022	0.09	0.45
	300	0.66	16.16	0.036	0.14	0.48
	400	0.88	23.66	0.052	0.21	0.53
	600	1.32	33.16	0.073	0.30	0.49
	800	1.76	46.16	0.102	0.41	0.51
					Avg	0.49
					Sd(n-1)	0.03
					n	6

Table 11 (cont'd)

B-B2	E, in	0.979				
	l, in	0.838				
	r _s , in	0.45425				
	d, in	4.048				
Run 5	CW	28 mm	White	PE foam	Non-glued	
	F _v , g	F _v , lb	F, g	F, lb	T, in-lb	μ _{cw}
	150	0.33	9.66	0.021	0.09	0.57
	200	0.44	10.16	0.022	0.09	0.45
	300	0.66	17.16	0.038	0.15	0.51
	400	0.88	21.66	0.048	0.19	0.48
	600	1.32	32.66	0.072	0.29	0.49
	800	1.76	45.66	0.101	0.41	0.51
					Avg	0.50
					Sd(n-1)	0.04
					n	6

B-B2	E, in	0.979				
	l, in	0.838				
	r _s , in	0.45425				
	d, in	4.048				
Run 5	CCW	28 mm	White	PE foam	Non-glued	
	F _v , g	F _v , lb	F, g	F, lb	T, in-lb	μ _{ccw}
	150	0.33	8.16	0.018	0.07	0.48
	200	0.44	11.66	0.026	0.10	0.52
	300	0.66	17.16	0.038	0.15	0.51
	400	0.88	21.16	0.047	0.19	0.47
	600	1.32	34.16	0.075	0.30	0.51
	800	1.76	47.16	0.104	0.42	0.53
					Avg	0.50
					Sd(n-1)	0.02
					n	6

Table 11 (cont'd)

B-B4	E, in	0.979		r_s , in	0.45425	
	l, in	0.838		d, in	4.048	
Run 1	CW	28 mm	Black	P/SF	Non-glued	
	F_v , g	F_v , lb	F, g	F, lb	T, in-lb	μ_{cw}
	600	1.32	11.16	0.025	0.10	0.17
	800	1.76	15.16	0.033	0.14	0.17
	1000	2.21	18.66	0.041	0.17	0.17
	1200	2.65	21.16	0.047	0.19	0.16
	1400	3.09	23.16	0.051	0.21	0.15
					Avg	0.16
					Sd(n-1)	0.01
					n	5

B-B4	E, in	0.979		r_s , in	0.45425	
	l, in	0.838		d, in	4.048	
Run 1	CCW	28 mm	Black	P/SF	Non-glued	
	F_v , g	F_v , lb	F, g	F, lb	T, in-lb	μ_{ccw}
	600	1.32	10.66	0.024	0.10	0.16
	800	1.76	13.66	0.030	0.12	0.15
	1000	2.21	17.16	0.038	0.15	0.15
	1200	2.65	20.16	0.044	0.18	0.15
	1400	3.09	22.66	0.050	0.20	0.14
					Avg	0.15
					Sd(n-1)	0.01
					n	5

B-B4	E, in	0.979		r_s , in	0.45425	
	l, in	0.838		d, in	4.048	
Run 2	CW	28 mm	Black	P/SF	Non-glued	
	F_v , g	F_v , lb	F, g	F, lb	T, in-lb	μ_{cw}
	600	1.32	10.16	0.022	0.09	0.15
	800	1.76	14.66	0.032	0.13	0.16
	1000	2.21	20.16	0.044	0.18	0.18
	1200	2.65	23.16	0.051	0.21	0.17
	1400	3.09	27.16	0.060	0.24	0.17
					Avg	0.17
					Sd(n-1)	0.01
					n	5

Table 11 (cont'd)

B-B4	E, in	0.979		r_s , in	0.45425	
	l, in	0.838		d, in	4.048	
Run 2	CCW	28 mm	Black	P/SF	Non-glued	
	F_v , g	F_v , lb	F, g	F, lb	T, in-lb	μ_{ccw}
	600	1.32	10.16	0.022	0.09	0.15
	800	1.76	14.66	0.032	0.13	0.16
	1000	2.21	19.66	0.043	0.18	0.18
	1200	2.65	23.16	0.051	0.21	0.17
	1400	3.09	28.66	0.063	0.26	0.18
					Avg	0.17
					Sd(n-1)	0.01
					n	5

B-B4	E, in	0.979		r_s , in	0.45425	
	l, in	0.838		d, in	4.048	
Run 3	CW	28 mm	Black	P/SF	Non-glued	
	F_v , g	F_v , lb	F, g	F, lb	T, in-lb	μ_{cw}
	600	1.32	10.16	0.022	0.09	0.15
	800	1.76	15.16	0.033	0.14	0.17
	1000	2.21	19.66	0.043	0.18	0.18
	1200	2.65	21.16	0.047	0.19	0.16
	1400	3.09	29.66	0.065	0.26	0.19
					Avg	0.17
					Sd(n-1)	0.01
					n	5

B-B4	E, in	0.979		r_s , in	0.45425	
	l, in	0.838		d, in	4.048	
Run 3	CCW	28 mm	Black	P/SF	Non-glued	
	F_v , g	F_v , lb	F, g	F, lb	T, in-lb	μ_{ccw}
	600	1.32	10.66	0.024	0.10	0.16
	800	1.76	14.66	0.032	0.13	0.16
	1000	2.21	17.16	0.038	0.15	0.15
	1200	2.65	18.16	0.040	0.16	0.13
	1400	3.09	22.16	0.049	0.20	0.14
					Avg	0.15
					Sd(n-1)	0.01
					n	5

Table 11 (cont'd)

B-B4	E, in	0.979		r _s , in	0.45425	
	l, in	0.838		d, in	4.048	
Run 4	CW	28 mm	Black	P/SF	Non-glued	
	F _v , g	F _v , lb	F, g	F, lb	T, in-lb	μ _{cw}
	600	1.32	9.66	0.021	0.09	0.14
	800	1.76	13.16	0.029	0.12	0.15
	1000	2.21	20.16	0.044	0.18	0.18
	1200	2.65	23.66	0.052	0.21	0.18
	1400	3.09	21.66	0.048	0.19	0.14
					Avg	0.16
					Sd(n-1)	0.02
					n	5

B-B4	E, in	0.979		r _s , in	0.45425	
	l, in	0.838		d, in	4.048	
Run 4	CCW	28 mm	Black	P/SF	Non-glued	
	F _v , g	F _v , lb	F, g	F, lb	T, in-lb	μ _{ccw}
	600	1.32	10.16	0.022	0.09	0.15
	800	1.76	14.66	0.032	0.13	0.16
	1000	2.21	19.16	0.042	0.17	0.17
	1200	2.65	22.66	0.050	0.20	0.17
	1400	3.09	24.66	0.054	0.22	0.16
					Avg	0.16
					Sd(n-1)	0.01
					n	5

B-B4	E, in	0.979		r _s , in	0.45425	
	l, in	0.838		d, in	4.048	
Run 5	CW	28 mm	Black	P/SF	Non-glued	
	F _v , g	F _v , lb	F, g	F, lb	T, in-lb	μ _{cw}
	600	1.32	10.66	0.024	0.10	0.16
	800	1.76	14.66	0.032	0.13	0.16
	1000	2.21	17.66	0.039	0.16	0.16
	1200	2.65	21.66	0.048	0.19	0.16
	1400	3.09	28.66	0.063	0.26	0.18
					Avg	0.16
					Sd(n-1)	0.01
					n	5

Table 11 (cont'd)

B-B4	E, in	0.979		r _s , in	0.45425	
	l, in	0.838		d, in	4.048	
Run 5	CCW	28 mm	Black	P/SF	Non-glued	
	F _v , g	F _v , lb	F, g	F, lb	T, in-lb	μ _{ccw}
	600	1.32	10.66	0.024	0.10	0.16
	800	1.76	14.16	0.031	0.13	0.16
	1000	2.21	19.16	0.042	0.17	0.17
	1200	2.65	19.16	0.042	0.17	0.14
	1400	3.09	32.16	0.071	0.29	0.20
					Avg	0.17
					Sd(n-1)	0.02
					n	5

B-B6	E, in	0.979		r _s , in	0.45425	
	l, in	0.838		d, in	4.048	
Run 1	CW	28 mm	Black	P/RVTLF	glued	
	F _v , g	F _v , lb	F, g	F, lb	T, in-lb	μ _{cw}
	600	1.32	12.16	0.027	0.11	0.18
	800	1.76	15.66	0.035	0.14	0.17
	1000	2.21	20.16	0.044	0.18	0.18
	1200	2.65	23.16	0.051	0.21	0.17
	1400	3.09	27.66	0.061	0.25	0.18
					Avg	0.18
					Sd(n-1)	0.004
					n	5

B-B6	E, in	0.979		r _s , in	0.45425	
	l, in	0.838		d, in	4.048	
Run 1	CCW	28 mm	Black	P/RVTLF	glued	
	F _v , g	F _v , lb	F, g	F, lb	T, in-lb	μ _{ccw}
	600	1.32	11.66	0.026	0.10	0.17
	800	1.76	16.16	0.036	0.14	0.18
	1000	2.21	20.66	0.046	0.18	0.18
	1200	2.65	23.16	0.051	0.21	0.17
	1400	3.09	26.66	0.059	0.24	0.17
					Avg	0.18
					Sd(n-1)	0.01
					n	5

Table 11 (cont'd)

B-B6	E, in	0.979		r _s , in	0.45425	
	l, in	0.838		d, in	4.048	
Run 2	CW	28 mm	Black	P/RVTLF	glued	
	F _v , g	F _v , lb	F, g	F, lb	T, in-lb	μ _{cw}
	600	1.32	13.16	0.029	0.12	0.20
	800	1.76	18.66	0.041	0.17	0.21
	1000	2.21	22.16	0.049	0.20	0.20
	1200	2.65	25.16	0.055	0.22	0.19
	1400	3.09	30.16	0.067	0.27	0.19
					Avg	0.20
					Sd(n-1)	0.01
					n	5

B-B6	E, in	0.979		r _s , in	0.45425	
	l, in	0.838		d, in	4.048	
Run 2	CCW	28 mm	Black	P/RVTLF	glued	
	F _v , g	F _v , lb	F, g	F, lb	T, in-lb	μ _{ccw}
	600	1.32	14.16	0.031	0.13	0.21
	800	1.76	18.66	0.041	0.17	0.21
	1000	2.21	23.16	0.051	0.21	0.21
	1200	2.65	25.66	0.057	0.23	0.19
	1400	3.09	30.66	0.068	0.27	0.20
					Avg	0.20
					Sd(n-1)	0.01
					n	5

B-B6	E, in	0.979		r _s , in	0.45425	
	l, in	0.838		d, in	4.048	
Run 3	CW	28 mm	Black	P/RVTLF	glued	
	F _v , g	F _v , lb	F, g	F, lb	T, in-lb	μ _{cw}
	600	1.32	12.16	0.027	0.11	0.18
	800	1.76	15.66	0.035	0.14	0.17
	1000	2.21	21.66	0.048	0.19	0.19
	1200	2.65	24.16	0.053	0.22	0.18
	1400	3.09	28.16	0.062	0.25	0.18
					Avg	0.18
					Sd(n-1)	0.01
					n	5

Table 11 (cont'd)

B-B6	E, in	0.979		r_s , in	0.45425	
	l, in	0.838		d, in	4.048	
Run 3	CCW	28 mm	Black	P/RVTLF	glued	
	F_v , g	F_v , lb	F, g	F, lb	T, in-lb	μ_{ccw}
	600	1.32	10.66	0.024	0.10	0.16
	800	1.76	15.66	0.035	0.14	0.17
	1000	2.21	21.16	0.047	0.19	0.19
	1200	2.65	26.16	0.058	0.23	0.19
	1400	3.09	26.16	0.058	0.23	0.17
					Avg	0.18
					Sd(n-1)	0.01
					n	5

B-B6	E, in	0.979		r_s , in	0.45425	
	l, in	0.838		d, in	4.048	
Run 4	CW	28 mm	Black	P/RVTLF	glued	
	F_v , g	F_v , lb	F, g	F, lb	T, in-lb	μ_{cw}
	600	1.32	10.66	0.024	0.10	0.16
	800	1.76	16.66	0.037	0.15	0.19
	1000	2.21	21.16	0.047	0.19	0.19
	1200	2.65	26.16	0.058	0.23	0.19
	1400	3.09	27.66	0.061	0.25	0.18
					Avg	0.18
					Sd(n-1)	0.01
					n	5

B-B6	E, in	0.979		r_s , in	0.45425	
	l, in	0.838		d, in	4.048	
Run 4	CCW	28 mm	Black	P/RVTLF	glued	
	F_v , g	F_v , lb	F, g	F, lb	T, in-lb	μ_{ccw}
	600	1.32	10.66	0.024	0.10	0.16
	800	1.76	15.66	0.035	0.14	0.17
	1000	2.21	18.16	0.040	0.16	0.16
	1200	2.65	24.16	0.053	0.22	0.18
	1400	3.09	27.16	0.060	0.24	0.17
					Avg	0.17
					Sd(n-1)	0.01
					n	5

Table 11 (cont'd)

B-B6	E, in	0.979		r _s , in	0.45425	
	l, in	0.838		d, in	4.048	
Run 5	CW	28 mm	Black	P/RVTLF	glued	
	F _v , g	F _v , lb	F, g	F, lb	T, in-lb	μ _{cw}
	600	1.32	10.16	0.022	0.09	0.15
	800	1.76	14.16	0.031	0.13	0.16
	1000	2.21	23.66	0.052	0.21	0.21
	1200	2.65	22.66	0.050	0.20	0.17
	1400	3.09	25.16	0.055	0.22	0.16
					Avg	0.17
					Sd(n-1)	0.02
					n	5

B-B6	E, in	0.979		r _s , in	0.45425	
	l, in	0.838		d, in	4.048	
Run 5	CCW	28 mm	Black	P/RVTLF	Glued	
	F _v , g	F _v , lb	F, g	F, lb	T, in-lb	μ _{ccw}
	600	1.32	11.16	0.025	0.10	0.17
	800	1.76	17.16	0.038	0.15	0.19
	1000	2.21	22.66	0.050	0.20	0.20
	1200	2.65	19.66	0.043	0.18	0.15
	1400	3.09	29.16	0.064	0.26	0.19
					Avg	0.18
					Sd(n-1)	0.02
					n	5

B-B7	E, in	0.979		r _s , in	0.45425	
	l, in	0.838		d, in	4.048	
Run 1	CW	28 mm	White	P/RVTLF	Non-glued	
	F _v , g	F _v , lb	F, g	F, lb	T, in-lb	μ _{cw}
	600	1.32	12.16	0.027	0.11	0.18
	800	1.76	17.16	0.038	0.15	0.19
	1000	2.21	23.16	0.051	0.21	0.21
	1200	2.65	27.16	0.060	0.24	0.20
	1400	3.09	30.16	0.067	0.27	0.19
					Avg	0.19
					Sd(n-1)	0.01
					n	5

Table 11 (cont'd)

B-B7	E, in	0.979		r_s , in	0.45425	
	l, in	0.838		d, in	4.048	
Run 1	CCW	28 mm	White	P/RVTLF	Non-glued	
	F_v , g	F_v , lb	F, g	F, lb	T, in-lb	μ_{ccw}
	600	1.32	11.16	0.025	0.10	0.17
	800	1.76	16.16	0.036	0.14	0.18
	1000	2.21	21.16	0.047	0.19	0.19
	1200	2.65	26.16	0.058	0.23	0.19
	1400	3.09	30.16	0.067	0.27	0.19
					Avg	0.18
					Sd(n-1)	0.01
					n	5

B-B7	E, in	0.979		r_s , in	0.45425	
	l, in	0.838		d, in	4.048	
Run 2	CW	28 mm	White	P/RVTLF	Non-glued	
	F_v , g	F_v , lb	F, g	F, lb	T, in-lb	μ_{cw}
	600	1.32	10.66	0.024	0.10	0.16
	800	1.76	15.16	0.033	0.14	0.17
	1000	2.21	19.16	0.042	0.17	0.17
	1200	2.65	22.66	0.050	0.20	0.17
	1400	3.09	26.66	0.059	0.24	0.17
					Avg	0.17
					Sd(n-1)	0.01
					n	5

B-B7	E, in	0.979		r_s , in	0.45425	
	l, in	0.838		d, in	4.048	
Run 2	CCW	28 mm	White	P/RVTLF	Non-glued	
	F_v , g	F_v , lb	F, g	F, lb	T, in-lb	μ_{ccw}
	600	1.32	10.16	0.022	0.09	0.15
	800	1.76	14.66	0.032	0.13	0.16
	1000	2.21	18.66	0.041	0.17	0.17
	1200	2.65	22.16	0.049	0.20	0.16
	1400	3.09	26.16	0.058	0.23	0.17
					Avg	0.16
					Sd(n-1)	0.01
					n	5

Table 11 (cont'd)

B-B7	E, in	0.979		r _s , in	0.45425	
	l, in	0.838		d, in	4.048	
Run 3	CW	28 mm	White	P/RVTLF	Non-glued	
	F _v , g	F _v , lb	F, g	F, lb	T, in-lb	μ _{cw}
	600	1.32	13.16	0.029	0.12	0.20
	800	1.76	16.66	0.037	0.15	0.19
	1000	2.21	19.66	0.043	0.18	0.18
	1200	2.65	23.66	0.052	0.21	0.18
	1400	3.09	27.66	0.061	0.25	0.18
					Avg	0.18
					Sd(n-1)	0.01
					n	5

B-B7	E, in	0.979		r _s , in	0.45425	
	l, in	0.838		d, in	4.048	
Run 3	CCW	28 mm	White	P/RVTLF	Non-glued	
	F _v , g	F _v , lb	F, g	F, lb	T, in-lb	μ _{ccw}
	600	1.32	12.16	0.027	0.11	0.18
	800	1.76	20.66	0.046	0.18	0.23
	1000	2.21	21.66	0.048	0.19	0.19
	1200	2.65	25.16	0.055	0.22	0.19
	1400	3.09	26.66	0.059	0.24	0.17
					Avg	0.19
					Sd(n-1)	0.02
					n	5

B-B7	E, in	0.979		r _s , in	0.45425	
	l, in	0.838		d, in	4.048	
Run 4	CW	28 mm	White	P/RVTLF	Non-glued	
	F _v , g	F _v , lb	F, g	F, lb	T, in-lb	μ _{cw}
	600	1.32	11.66	0.026	0.10	0.17
	800	1.76	17.66	0.039	0.16	0.20
	1000	2.21	19.16	0.042	0.17	0.17
	1200	2.65	24.16	0.053	0.22	0.18
	1400	3.09	30.16	0.067	0.27	0.19
					Avg	0.18
					Sd(n-1)	0.01
					n	5

Table 11 (cont'd)

B-B7	E, in	0.979		r _s , in	0.45425	
	l, in	0.838		d, in	4.048	
Run 4	CCW	28 mm	White	P/RVTLF	Non-glued	
	F _v , g	F _v , lb	F, g	F, lb	T, in-lb	μ _{ccw}
	600	1.32	10.66	0.024	0.10	0.16
	800	1.76	14.66	0.032	0.13	0.16
	1000	2.21	22.66	0.050	0.20	0.20
	1200	2.65	25.66	0.057	0.23	0.19
	1400	3.09	29.66	0.065	0.26	0.19
					Avg	0.18
					Sd(n-1)	0.02
					n	5

B-B7	E, in	0.979		r _s , in	0.45425	
	l, in	0.838		d, in	4.048	
Run 5	CW	28 mm	White	P/RVTLF	Non-glued	
	F _v , g	F _v , lb	F, g	F, lb	T, in-lb	μ _{cw}
	600	1.32	13.16	0.029	0.12	0.20
	800	1.76	14.16	0.031	0.13	0.16
	1000	2.21	20.16	0.044	0.18	0.18
	1200	2.65	23.16	0.051	0.21	0.17
	1400	3.09	32.66	0.072	0.29	0.21
					Avg	0.18
					Sd(n-1)	0.02
					n	5

B-B7	E, in	0.979		r _s , in	0.45425	
	l, in	0.838		d, in	4.048	
Run 5	CCW	28 mm	White	P/RVTLF	Non-glued	
	F _v , g	F _v , lb	F, g	F, lb	T, in-lb	μ _{ccw}
	600	1.32	10.16	0.022	0.09	0.15
	800	1.76	16.16	0.036	0.14	0.18
	1000	2.21	20.66	0.046	0.18	0.18
	1200	2.65	26.16	0.058	0.23	0.19
	1400	3.09	30.66	0.068	0.27	0.20
					Avg	0.18
					Sd(n-1)	0.02
					n	5

Table 11 (cont'd)

C-C1	E, in	1.3605		r _s , in	0.64538	
	l, in	1.221		d, in	4.048	
Run 1	CW	38 mm	White	PE foam	glued	
	F _v , g	F _v , lb	F, g	F, lb	T, in-lb	μ _{cw}
	200	0.44	13.66	0.030	0.12	0.43
	300	0.66	19.66	0.043	0.18	0.41
	400	0.88	24.66	0.054	0.22	0.39
	600	1.32	41.16	0.091	0.37	0.43
	800	1.76	52.66	0.116	0.47	0.41
					Avg	0.41
					Sd(n-1)	0.02
					n	5

C-C1	E, in	1.3605		r _s , in	0.64538	
	l, in	1.221		d, in	4.048	
Run 1	CCW	38 mm	White	PE foam	glued	
	F _v , g	F _v , lb	F, g	F, lb	T, in-lb	μ _{ccw}
	200	0.44	14.66	0.032	0.13	0.46
	300	0.66	21.16	0.047	0.19	0.44
	400	0.88	27.16	0.060	0.24	0.43
	600	1.32	45.16	0.100	0.40	0.47
	800	1.76	60.16	0.133	0.54	0.47
					Avg	0.45
					Sd(n-1)	0.02
					n	5

C-C1	E, in	1.3605		r _s , in	0.64538	
	l, in	1.221		d, in	4.048	
Run 2	CW	38 mm	White	PE foam	glued	
	F _v , g	F _v , lb	F, g	F, lb	T, in-lb	μ _{cw}
	200	0.44	15.66	0.035	0.14	0.49
	300	0.66	22.66	0.050	0.20	0.47
	400	0.88	31.16	0.069	0.28	0.49
	600	1.32	48.66	0.107	0.43	0.51
	800	1.76	62.16	0.137	0.55	0.49
					Avg	0.49
					Sd(n-1)	0.01
					n	5

Table 11 (cont'd)

C-C1	E, in	1.3605		r _s , in	0.64538	
	l, in	1.221		d, in	4.048	
Run 2	CCW	38 mm	White	PE foam	glued	
	F _v , g	F _v , lb	F, g	F, lb	T, in-lb	μ _{ccw}
	200	0.44	18.16	0.040	0.16	0.57
	300	0.66	26.16	0.058	0.23	0.55
	400	0.88	33.16	0.073	0.30	0.52
	600	1.32	52.16	0.115	0.47	0.55
	800	1.76	66.16	0.146	0.59	0.52
					Avg	0.54
					Sd(n-1)	0.02
					n	5

C-C1	E, in	1.3605		r _s , in	0.64538	
	l, in	1.221		d, in	4.048	
Run 3	CW	38 mm	White	PE foam	glued	
	F _v , g	F _v , lb	F, g	F, lb	T, in-lb	μ _{cw}
	200	0.44	18.16	0.040	0.16	0.57
	300	0.66	19.16	0.042	0.17	0.40
	400	0.88	30.16	0.067	0.27	0.47
	600	1.32	46.66	0.103	0.42	0.49
	800	1.76	65.16	0.144	0.58	0.51
					Avg	0.49
					Sd(n-1)	0.06
					n	5

C-C1	E, in	1.3605		r _s , in	0.64538	
	l, in	1.221		d, in	4.048	
Run 3	CCW	38 mm	White	PE foam	glued	
	F _v , g	F _v , lb	F, g	F, lb	T, in-lb	μ _{ccw}
	200	0.44	18.66	0.041	0.17	0.59
	300	0.66	21.16	0.047	0.19	0.44
	400	0.88	31.66	0.070	0.28	0.50
	600	1.32	51.16	0.113	0.46	0.53
	800	1.76	63.66	0.140	0.57	0.50
					Avg	0.51
					Sd(n-1)	0.05
					n	5

Table 11 (cont'd)

C-C1	E, in	1.3605		r _s , in	0.64538	
	l, in	1.221		d, in	4.048	
Run 4	CW	38 mm	White	PE foam	glued	
	F _v , g	F _v , lb	F, g	F, lb	T, in-lb	μ _{cw}
	200	0.44	14.16	0.031	0.13	0.44
	300	0.66	22.66	0.050	0.20	0.47
	400	0.88	27.66	0.061	0.25	0.43
	600	1.32	43.16	0.095	0.39	0.45
	800	1.76	54.66	0.121	0.49	0.43
					Avg	0.45
					Sd(n-1)	0.02
					n	5

C-C1	E, in	1.3605		r _s , in	0.64538	
	l, in	1.221		d, in	4.048	
Run 4	CCW	38 mm	White	PE foam	glued	
	F _v , g	F _v , lb	F, g	F, lb	T, in-lb	μ _{ccw}
	200	0.44	14.66	0.032	0.13	0.46
	300	0.66	17.16	0.038	0.15	0.36
	400	0.88	26.16	0.058	0.23	0.41
	600	1.32	44.66	0.098	0.40	0.47
	800	1.76	70.16	0.155	0.63	0.55
					Avg	0.45
					Sd(n-1)	0.07
					n	5

C-C1	E, in	1.3605		r _s , in	0.64538	
	l, in	1.221		d, in	4.048	
Run 5	CW	38 mm	White	PE foam	Glued	
	F _v , g	F _v , lb	F, g	F, lb	T, in-lb	μ _{cw}
	200	0.44	17.16	0.038	0.15	0.54
	300	0.66	19.16	0.042	0.17	0.40
	400	0.88	29.66	0.065	0.26	0.47
	600	1.32	38.66	0.085	0.35	0.40
	800	1.76	57.16	0.126	0.51	0.45
					Avg	0.45
					Sd(n-1)	0.06
					N	5

Table 11 (cont'd)

C-C1	E, in	1.3605		r_s , in	0.64538	
	l, in	1.221		d, in	4.048	
Run 5	CCW	38 mm	White	PE foam	Glued	
	F_v , g	F_v , lb	F, g	F, lb	T, in-lb	μ_{ccw}
	200	0.44	16.66	0.037	0.15	0.52
	300	0.66	20.16	0.044	0.18	0.42
	400	0.88	24.66	0.054	0.22	0.39
	600	1.32	49.16	0.108	0.44	0.51
	800	1.76	66.16	0.146	0.59	0.52
					Avg	0.47
					Sd(n-1)	0.06
					N	5

C-C2	E, in	1.3605		r_s , in	0.64538	
	l, in	1.221		d, in	4.048	
Run 1	CW	38 mm	White	PE foam	Non-glued	
	F_v , g	F_v , lb	F, g	F, lb	T, in-lb	μ_{cw}
	300	0.66	9.66	0.021	0.09	0.20
	400	0.88	12.16	0.027	0.11	0.19
	600	1.32	20.16	0.044	0.18	0.21
	800	1.76	46.16	0.102	0.41	0.36
	1000	2.21	61.16	0.135	0.55	0.38
					Avg	0.27
					Sd(n-1)	0.09
					N	5

C-C2	E, in	1.3605		r_s , in	0.64538	
	l, in	1.221		d, in	4.048	
Run 1	CCW	38 mm	White	PE foam	Non-glued	
	F_v , g	F_v , lb	F, g	F, lb	T, in-lb	μ_{ccw}
	300	0.66	12.66	0.028	0.11	0.26
	400	0.88	19.16	0.042	0.17	0.30
	600	1.32	26.16	0.058	0.23	0.27
	800	1.76	46.16	0.102	0.41	0.36
	1000	2.21	61.16	0.135	0.55	0.38
					Avg	0.32
					Sd(n-1)	0.05
					N	5

Table 11 (cont'd)

C-C2	E, in	1.3605		r _s , in	0.64538	
	l, in	1.221		d, in	4.048	
Run 2	CW	38 mm	White	PE foam	Non-glued	
	F _v , g	F _v , lb	F, g	F, lb	T, in-lb	μ _{cw}
	300	0.66	18.16	0.040	0.16	0.38
	400	0.88	26.16	0.058	0.23	0.41
	600	1.32	38.16	0.084	0.34	0.40
	800	1.76	48.16	0.106	0.43	0.38
	1000	2.21	61.16	0.135	0.55	0.38
					Avg	0.39
					Sd(n-1)	0.01
					n	5

C-C2	E, in	1.3605		r _s , in	0.64538	
	l, in	1.221		d, in	4.048	
Run 2	CCW	38 mm	White	PE foam	Non-glued	
	F _v , g	F _v , lb	F, g	F, lb	T, in-lb	μ _{ccw}
	300	0.66	17.16	0.038	0.15	0.36
	400	0.88	26.16	0.058	0.23	0.41
	600	1.32	40.16	0.089	0.36	0.42
	800	1.76	50.16	0.111	0.45	0.39
	1000	2.21	62.16	0.137	0.55	0.39
					Avg	0.39
					Sd(n-1)	0.02
					n	5

C-C2	E, in	1.3605		r _s , in	0.64538	
	l, in	1.221		d, in	4.048	
Run 3	CW	38 mm	White	PE foam	Non-glued	
	F _v , g	F _v , lb	F, g	F, lb	T, in-lb	μ _{cw}
	300	0.66	15.16	0.033	0.14	0.32
	400	0.88	25.16	0.055	0.22	0.39
	600	1.32	36.66	0.081	0.33	0.38
	800	1.76	49.16	0.108	0.44	0.39
	1000	2.21	61.66	0.136	0.55	0.39
					Avg	0.37
					Sd(n-1)	0.03
					n	5

Table 11 (cont'd)

C-C2	E, in	1.3605		r _s , in	0.64538	
	l, in	1.221		d, in	4.048	
Run 3	CCW	38 mm	White	PE foam	Non-glued	
	F _v , g	F _v , lb	F, g	F, lb	T, in-lb	μ _{ccw}
	300	0.66	16.16	0.036	0.14	0.34
	400	0.88	23.16	0.051	0.21	0.36
	600	1.32	40.16	0.089	0.36	0.42
	800	1.76	46.66	0.103	0.42	0.37
	1000	2.21	61.66	0.136	0.55	0.39
					Avg	0.37
					Sd(n-1)	0.03
					n	5

C-C2	E, in	1.3605		r _s , in	0.64538	
	l, in	1.221		d, in	4.048	
Run 4	CW	38 mm	White	PE foam	Non-glued	
	F _v , g	F _v , lb	F, g	F, lb	T, in-lb	μ _{cw}
	300	0.66	15.66	0.035	0.14	0.33
	400	0.88	24.16	0.053	0.22	0.38
	600	1.32	38.16	0.084	0.34	0.40
	800	1.76	46.16	0.102	0.41	0.36
	1000	2.21	61.16	0.135	0.55	0.38
					Avg	0.37
					Sd(n-1)	0.03
					n	5

C-C2	E, in	1.3605		r _s , in	0.64538	
	l, in	1.221		d, in	4.048	
Run 4	CCW	38 mm	White	PE foam	Non-glued	
	F _v , g	F _v , lb	F, g	F, lb	T, in-lb	μ _{ccw}
	300	0.66	18.66	0.041	0.17	0.39
	400	0.88	21.66	0.048	0.19	0.34
	600	1.32	39.66	0.087	0.35	0.41
	800	1.76	46.16	0.102	0.41	0.36
	1000	2.21	61.66	0.136	0.55	0.39
					Avg	0.38
					Sd(n-1)	0.03
					n	5

Table 11 (cont'd)

C-C2	E, in	1.3605		r_s , in	0.64538	
	l, in	1.221		d, in	4.048	
Run 5	CW	38 mm	White	PE foam	Non-glued	
	F_v , g	F_v , lb	F, g	F, lb	T, in-lb	μ_{cw}
	300	0.66	17.66	0.039	0.16	0.37
	400	0.88	24.16	0.053	0.22	0.38
	600	1.32	39.66	0.087	0.35	0.41
	800	1.76	48.16	0.106	0.43	0.38
	1000	2.21	61.16	0.135	0.55	0.38
					Avg	0.38
					Sd(n-1)	0.02
					n	5

C-C2	E, in	1.3605		r_s , in	0.64538	
	l, in	1.221		d, in	4.048	
Run 5	CCW	38 mm	White	PE foam	Non-glued	
	F_v , g	F_v , lb	F, g	F, lb	T, in-lb	μ_{ccw}
	300	0.66	18.66	0.041	0.17	0.39
	400	0.88	23.16	0.051	0.21	0.36
	600	1.32	32.66	0.072	0.29	0.34
	800	1.76	49.16	0.108	0.44	0.39
	1000	2.21	60.16	0.133	0.54	0.38
					Avg	0.37
					Sd(n-1)	0.02
					n	5

Table 12 Raw Data of the Measured Application Torque and Instantaneous Removal Torque

B-B1			B-B2			B-B3		
Rep	AT	ISRT	Rep	AT	ISRT	Rep	AT	ISRT
1	13.9	7.1	1	14	12.1	1	14.1	10.6
2	13.9	6.3	2	14.6	11	2	14.4	11.1
3	13.7	7.7	3	14.1	10	3	14.2	10.6
4	13.8	6.5	4	13.9	10.9	4	14.7	10
5	13.9	5.4	5	13.8	11.8	5	13.5	10.7
Avg	13.84	6.6	avg	14.08	11.16	avg	14.18	10.6
Sd	0.09	0.87	sd	0.31	0.83	sd	0.44	0.39
ISRT/AT	0.4769		ISRT/A T	0.7926		ISRT/A T	0.7475	

B-B4			B-B5			B-B6		
Rep	AT	ISRT	Rep	AT	ISRT	Rep	AT	ISRT
1	14	10.8	1	14	13.6	1	13.9	9.7
2	13.8	11.3	2	14	13.4	2	14.3	8.8
3	14.4	11.3	3	14	12.6	3	14.1	10
4	13.9	11.6	4	14.2	11.8	4	14.1	10.7
5	14.4	11.1	5	14.2	12.6	5	14.3	9.6
Avg	14.1	11.22	avg	14.08	12.8	avg	14.14	9.76
Sd	0.28	0.29	sd	0.11	0.72	sd	0.17	0.69
ISRT/AT	0.7957		ISRT/A T	0.9091		ISRT/A T	0.6902	

B-B7			B-B8		
Rep	AT	ISRT	Rep	AT	ISRT
1	14.2	12.4	1	14.2	12.8
2	14.3	12.9	2	14	11
3	14	13	3	14	12.4
4	14	12.6	4	14.2	10.7
5	14.2	12.8	5	14	10.4
Avg	14.14	12.74	avg	14.08	11.46
Sd	0.13	0.24	sd	0.11	1.07
ISRT/A T	0.9010		ISRT/A T	0.8139	

Table 12 (cont'd)

C-C1			C-C2		
Rep	AT	ISRT	Rep	AT	ISRT
1	19.2	10.5	1	18.8	16.3
2	19.4	13.1	2	18.9	16.6
3	19.7	13.1	3	18.9	16.3
4	19.2	14.4	4	18.9	16
5	19	10.1	5	19.2	16.2
Avg	19.3	12.24	avg	18.94	16.28
Sd	0.26	1.85	sd	0.15	0.22
ISRT/AT	0.6342		ISRT/A T	0.8596	

Table 13 Raw Data of the Measured Application Torque and Immediate Removal Torque

B-B1			B-B2			B-B3		
Rep	AT	IRT	Rep	AT	IRT	Rep	AT	IRT
1	14	5.7	1	14.1	10.1	1	13.8	9.2
2	14	5.8	2	14	9.2	2	13.9	8.7
3	13.8	6.3	3	14.6	9.2	3	13.9	9.1
4	14	7.5	4	13.9	8.7	4	14.4	8.9
5	14	6.5	5	14.2	9.2	5	14.2	9.2
avg	13.96	6.36	avg	14.16	9.28	avg	14.04	9.02
sd	0.09	0.72	sd	0.27	0.51	sd	0.25	0.22
IRT/AT	0.4556		IRT/AT	0.6554		IRT/AT	0.6425	

B-B4			B-B5			B-B6			k
Rep	AT	IRT	Rep	AT	IRT	Rep	AT	IRT	0.7387
1	14	9.3	1	14.1	9.3	1	13.8	9.5	
2	14.1	8.1	2	13.9	8	2	14.2	8.4	
3	14.2	8	3	13.9	9.5	3	13.8	8.4	
4	14.2	8.2	4	13.9	9	4	14.3	8.1	
5	14	8.7	5	13.8	9.1	5	14	8.9	
avg	14.1	8.46	avg	13.92	8.98	avg	14.02	8.66	
sd	0.10	0.54	sd	0.11	0.58	sd	0.23	0.55	
IRT/AT	0.6000		IRT/AT	0.6451		IRT/AT	0.6177		

B-B7			B-B8		
Rep	AT	IRT	Rep	AT	IRT
1	13.9	10.2	1	13.8	10.5
2	13.7	9.2	2	13.8	10.2
3	13.8	10	3	14	10.7
4	14.1	8.6	4	13.9	8.6
5	13.9	10.6	5	14.3	9.4
avg	13.88	9.72	avg	13.96	9.88
sd	0.15	0.81	sd	0.21	0.87
IRT/AT	0.7003		IRT/AT	0.7077	

Table 13 (cont'd)

C-C1			C-C2		
Rep	AT	IRT	Rep	AT	IRT
1	19.4	8.6	1	19.3	12.2
2	19	9.1	2	19.4	13
3	19.4	9.9	3	18.6	12.9
4	18.9	9.1	4	19.7	13.5
5	18.8	9	5	19.3	13.2
avg	19.1	9.14	avg	19.26	12.96
sd	0.28	0.47	sd	0.40	0.48
IRT/AT	0.4785		IRT/AT	0.6729	

Table 14 The Predicted Removal Torque, T' Calculated Using AT from Table 12

Rep	B-B1	B-B2	B-B3	B-B4	B-B5	B-B6	B-B7	B-B8	C-C1	C-C2
1	12.29	12.41	12.23	10.50	10.57	10.19	10.55	10.48	16.99	16.44
2	12.29	12.94	12.32	10.57	10.42	10.49	10.40	10.48	16.64	16.52
3	12.11	12.50	12.32	10.65	10.42	10.19	10.48	10.63	16.99	15.84
4	12.20	12.32	12.76	10.65	10.42	10.56	10.70	10.55	16.55	16.78
5	12.29	12.23	12.59	10.50	10.35	10.34	10.55	10.86	16.46	16.44
Avg	12.23	12.48	12.45	10.57	10.44	10.36	10.54	10.60	16.72	16.40
Sd	0.08	0.28	0.22	0.07	0.08	0.17	0.11	0.16	0.25	0.34

Note: T' ± 26%

Table 15 The Predicted Removal Torque, T' Calculated Using AT from Table 13

Rep	B-B1	B-B2	B-B3	B-B4	B-B5	B-B6	B-B7	B-B8	C-C1	C-C2
1	12.37	12.50	12.50	10.50	10.50	10.27	10.78	10.78	16.81	16.01
2	12.37	12.41	12.76	10.35	10.50	10.56	10.86	10.63	16.99	16.10
3	12.20	12.94	12.59	10.80	10.50	10.42	10.63	10.63	17.25	16.10
4	12.37	12.32	13.03	10.42	10.65	10.42	10.63	10.78	16.81	16.10
5	12.37	12.59	11.97	10.80	10.65	10.56	10.78	10.63	16.64	16.35
Avg	12.34	12.55	12.57	10.57	10.56	10.44	10.74	10.69	16.90	16.13
Sd	0.08	0.24	0.39	0.21	0.08	0.12	0.10	0.08	0.23	0.13

Note: T' ± 26%

Table 16 k_a and k_r for Equations (18) and (19)

Treatment	k_a	k_r
B-B1	0.48	0.42
B-B2	0.49	0.44
B-B3	0.49	0.44
B-B4	0.22	0.17
B-B5	0.22	0.17
B-B6	0.21	0.16
B-B7	0.23	0.18
B-B8	0.23	0.18
C-C1	0.44	0.38
C-C2	0.37	0.31

Note: k_a and $k_r \pm 26\%$

BIBLIOGRAPHY

BIBLIOGRAPHY

1. A Tekni-Plex Co. What is Tri-Seal?. [Online] Available <http://www.tri-seal.com>, December 2, 1999.
2. Birley, Arthur W., Haworth, Barry, and Batchelor, Jim, Physics of Plastics, Hanser Publisher.
3. Closure Manufacturers Association, Closure Guides. Washington D.C. 1993.
4. Crawford, Brian, Choosing the Right Closure Liner, Reprinted from Food & Drug Packaging.
5. Hanlon, Joseph F., Handbook of Package Engineering, Second Edition, Technomic publication, Lancaster PA, 1984.
6. McCarthy, Robert V., Performance of Plastic Screw Thread Attachment. M.S. Thesis, Franklin and Marshall College, Lancaster, Pennsylvania, 1956.
7. Nielsen, Lawrence E. and Landel, Robert F., Mechanical Properties of Polymer and Composites, Second Edition, Marcel Dekker, Inc., 1994.
8. Rearick, Paul W., Difference in Torque Measurements Taken by Manual and by Automatic Cap Torque Equipment. M.S. Thesis, School of Packaging, Michigan State University, 1995.
9. Soroka, Walter, Fundamentals of Packaging Technology, Institute of Packaging Professionals, Herndon, Virginia, 1995.
10. Soutas-Little, Robert W. and Inman, Daniel J., Engineering Mechanics Statics, Prentice Hall, Upper Saddle River, NJ, 1999.